

UNCERTAINTY PROPAGATION IN HYPERSONIC FLIGHT DYNAMICS  
AND COMPARISON OF DIFFERENT METHODS

A Thesis

by

AVINASH PRABHAKAR

Submitted to the Office of Graduate Studies of  
Texas A&M University  
in partial fulfillment of the requirements for the degree of

MASTER OF SCIENCE

December 2008

Major Subject: Aerospace Engineering

UNCERTAINTY PROPAGATION IN HYPERSONIC FLIGHT DYNAMICS  
AND COMPARISON OF DIFFERENT METHODS

A Thesis

by

AVINASH PRABHAKAR

Submitted to the Office of Graduate Studies of  
Texas A&M University  
in partial fulfillment of the requirements for the degree of

MASTER OF SCIENCE

Approved by:

Chair of Committee, Raktim Bhattacharya  
Committee Members, Suman Chakravorty  
Bani Mallick

Head of Department, Helen Reed

December 2008

Major Subject: Aerospace Engineering

## ABSTRACT

Uncertainty Propagation in Hypersonic Flight Dynamics  
and Comparison of Different Methods. (December 2008)

Avinash Prabhakar,

B.Eng., Indian Institute of Technology, Roorkee

Chair of Advisory Committee: Dr. Raktim Bhattacharya

In this work we present a novel computational framework for analyzing evolution of uncertainty in state trajectories of a hypersonic air vehicle due to uncertainty in initial conditions and other system parameters. The framework is built on the so called generalized Polynomial Chaos expansions. In this framework, stochastic dynamical systems are transformed into equivalent deterministic dynamical systems in higher dimensional space. In the research presented here we study evolution of uncertainty due to initial condition, ballistic coefficient, lift over drag ratio and atmospheric density.

We compute the statistics using the continuous linearization (CL) approach. This approach computes the jacobian of the perturbational variables about the nominal trajectory. The covariance is then propagated using the riccati equation and the statistics is compared with the Polynomial Chaos method. The latter gives better accuracy as compared to the CL method.

The simulation is carried out assuming uniform distribution on the parameters (initial condition, density, ballistic coefficient and lift over drag ratio). The method is

then extended for Gaussian distribution on the parameters and the statistics, mean and variance of the states are matched with the standard Monte Carlo methods. The problem studied here is related to the Mars entry descent landing problem.

To my parents and teachers for their guidance and encouragement

## ACKNOWLEDGMENTS

I would like to express my sincere thanks to Dr. Raktim Bhattacharya, Chair of my Advisory Committee, for introducing me to the amazing field of uncertainty analysis and estimation theory and lending his invaluable suggestions and guidance throughout my research. It was a learning experience for me especially in the context of getting practical and applicable results with the application of theories. I also thank him for providing an open and cordial atmosphere during our interactions and discussions. Further, I am also thankful to the members of my advisory committee, Dr. Suman Chakravorty and Dr. Bani Mallick for providing helpful suggestions and for reviewing my thesis.

The opportunity to work with the CISAR team has been a learning and enriching experience. In particular, I would like to thank Prasenjeet Sengupta, Baljeet Singh and James Fisher for their guidance and helpful discussions on various topics.

Finally, it is a pleasure to acknowledge my parents and friends for their encouraging support and patience throughout my study without which it would have been impossible for me to have completed the work.

## TABLE OF CONTENTS

CHAPTER		Page
I	INTRODUCTION . . . . .	1
	A. Problem Statement . . . . .	1
	B. Approach . . . . .	3
II	POLYNOMIAL CHAOS . . . . .	5
	A. Generalized Polynomial Chaos . . . . .	5
	B. Approximate Solution of Stochastic Differential Equations	6
	C. Stochastic Dynamics and Polynomial Chaos . . . . .	7
	D. Limitations of Polynomial Chaos . . . . .	11
III	VINH'S EQUATION WITH PROBABILISTIC UNCERTAINTY ON SYSTEM PARAMETERS . . . . .	13
	A. Obtaining Statistics from Polynomial Chaos . . . . .	18
	1. Uncertainty Propagation Using the Standard Ap- proach of Monte Carlo Simulations . . . . .	19
	B. Simulation Results for the Moments Propagation Using Polynomial Chaos Theory . . . . .	21
IV	CONTINUOUS LINEARIZATION APPROACH AND DOWN- RANGE ANALYSIS . . . . .	28
	A. Simulation Results . . . . .	31
	B. State Acquisition . . . . .	31
V	SUMMARY AND CONCLUSIONS . . . . .	39
	A. Summary . . . . .	39
	B. Future Work . . . . .	40
	REFERENCES . . . . .	43
	APPENDIX A . . . . .	45
	APPENDIX B . . . . .	46
	APPENDIX C . . . . .	53

CHAPTER	Page
APPENDIX D . . . . .	58
VITA . . . . .	61



## LIST OF TABLES

TABLE		Page
I	Correspondence between choice of polynomials and given distribution of $\Delta(\omega)$ . . . . .	6
II	Parameters for a Mars atmospheric entry vehicle. . . . .	14

## LIST OF FIGURES

FIGURE	Page
1      Uncertainty in initial condition. . . . .	2
2      Uncertainty in landing site. . . . .	3
3      Uncertainty in parameters for a dynamic model. . . . .	3
4      Evolution of Monte Carlo(blue) and Polynomial Chaos(green and red) trajectories with time. With higher order of expansions Polynomial Chaos trajectory approaches the Monte Carlo trajectory. . . . .	12
5      Planar 3 dimensional Vinh's equation is used for modeling the dynamics. Here the states are height(h), velocity(v), flight path angle ( $\gamma$ ). The states(h, v) are non dimensionalized using the radius of the planet( $R_0$ ), and the escape velocity( $v_e$ ) . . . . .	13
6      Evolution of uncertainty using 5% uniform uncertainty on initial conditions of state $h_0$ . The solid black trajectory is the mean trajectory. . . . .	21
7      Evolution of uncertainty using 5% uniform uncertainty on initial conditions of state $v_0$ . Evolution of uncertainty is more predominant in this case. The solid black trajectory is the mean trajectory. . . . .	22
8      Evolution of uncertainty using 5% uniform uncertainty on initial conditions of state $\gamma_0$ . The solid black trajectory is the mean trajectory. . . . .	23
9      Evolution of uncertainty using 5% uniform uncertainty on density ( $\rho_0$ ). . . . .	23
10     Evolution of uncertainty using 5% uniform uncertainty on Ballistic Constant( $B_c$ ) ratio. . . . .	24
11     Evolution of uncertainty using 5% uniform uncertainty on L over D ratio( $\nu_0$ ). We notice that the evolution of uncertainty is more in this case as compared to other parameters as $B_c$ and $\rho_0$ . . . . .	24

FIGURE	Page
12	Matching the moments, mean and variance, using 5% uniform uncertainty on $h_0$ using the Sampling Method. Blue trajectory is from Monte Carlo method and red dashed is obtained from Polynomial Chaos method. . . . . 25
13	Matching the moments, mean and variance, using 5% uniform uncertainty on $v_0$ using the Sampling Method. Blue trajectory is from Monte Carlo method and red dashed is obtained from Polynomial Chaos method. . . . . 25
14	Matching the moments, mean and variance, using 5% uniform uncertainty on $\gamma_0$ using the Sampling Method. Blue trajectory is from Monte Carlo method and red dashed is obtained from Polynomial Chaos method. . . . . 26
15	Matching the moments, mean and variance, using 5% uniform uncertainty on $\rho_0$ using the Sampling Method. . . . . 26
16	Comparing the error in moments (mean and variance) using 5% uniform uncertainty on $\rho_0$ and using the Sampling Method. Here the order of truncation is varied to see the convergence of the errors. 27
17	Matching the moments, mean and variance, using 5% Gaussian uncertainty on IC for the three approaches (MC, PC, CL). . . . . 34
18	Matching the moments, mean and variance, using 5% Gaussian uncertainty on IC and $\rho_0$ for the three approaches (MC, PC, CL). . . 35
19	Matching the moments, mean and variance, using 5% Gaussian uncertainty on IC and L over $D(\nu)$ ratio for the three approaches (MC, PC, CL). . . . . 37
20	Matching the moments, mean and variance, using 5% Gaussian uncertainty on IC and Bc ratio for the three approaches (MC, PC, CL). 38
21	Evolution of the dynamics using statistical linearization method. The simulation is run with starting statistics of mean 0.5 and variance of 1. . . . . 51

FIGURE	Page
22	Evolution of the PDF using the Fokker Plank Equation. The simulation is run with starting statistics of mean 0.5 and standard deviation of 0.01. . . . . 52
23	Numerical values of the coefficients of Hermite Chaos expansion used for capturing exponential distribution. . . . . 56
24	Evolution of Monte Carlo and Polynomial Chaos trajectory with time. The results match and the divergence over the period of time is due to long term integration issues of Polynomial Chaos method. . . . . 60

## CHAPTER I

### INTRODUCTION

#### A. Problem Statement

NASA has clearly identified the need for fundamental research on entry, descent, and landing of large robotic and manned spacecraft ( $> 30$  MT) on the surface of Mars with high accuracy. The expected mass of the next Mars Science Laboratory mission is approximately 2,800 kg at entry. The mission includes plans for a precision guided entry and a tether-based payload deployment system, which is expected to provide a landing accuracy of 20 – 40 km, from the target. Another major concern with high-mass entry is the mismatch between the entry conditions and the deceleration capabilities provided by supersonic parachute technologies. In such applications, there is uncertainty present in initial condition and other system parameters. Hence, for successful mission, it is critical to study the impact of such uncertainties on state trajectories and determine uncertainty in the landing site and the entry condition for super sonic parachute deployment. Figures 1 and 2 shows how the uncertainty on initial condition effects the uncertainty on landing site. Figure 3 summarizes the research problem addressed in this work. The figure clearly shows that the uncertainty on parameters like initial conditions and mass induces uncertainty on the final state of the dynamics.

The problem of studying the evolution of uncertainty in dynamical systems has been of interest consistently in the scientific community. In many cases, the uncertainty in initial condition and other system parameters for a dynamical system are not known

---

The journal model is *IEEE Transactions on Automatic Control*.

precisely. However, characteristics of the uncertainty, such as mean, standard deviation, probability density function, etc., may be known. A common technique to study the evolution of such distributions is the Monte-Carlo simulation. In this approach, a set of initial conditions that best represent the distribution, are propagated over the desired time interval, and statistical properties of the envelope of trajectories are studied. For example, the expected value of the set of trajectories may be evaluated easily, once all the trajectories are known. However, Monte-Carlo simulations are essentially brute force in nature, with the understanding that a large number of points may be required to accurately represent the distribution on initial conditions. As a consequence, the time required for computation is greatly affected by the dimension of the system and the desired accuracy of the result. Other alternatives include Gaussian closure of the parametric uncertainty and analysis of its impact by means of linear analysis. For nonlinear systems, this is achieved by continuous linearization. Such methods are known not to work well when nonlinearities are significant.

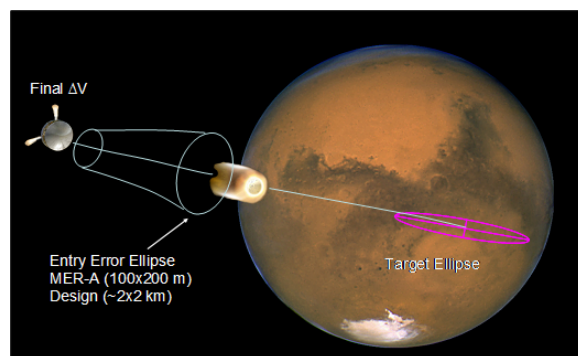


Fig. 1. Uncertainty in initial condition.

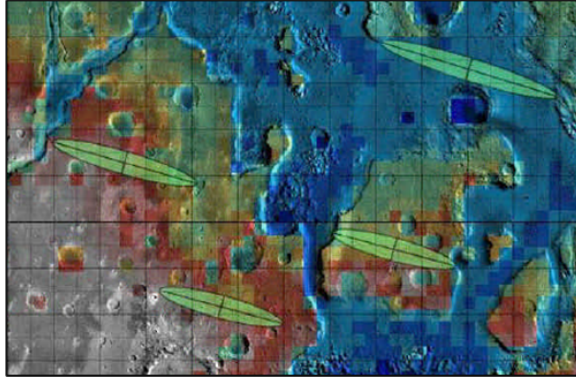


Fig. 2. Uncertainty in landing site.

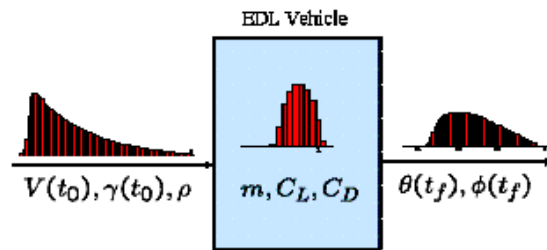


Fig. 3. Uncertainty in parameters for a dynamic model.

## B. Approach

In this research effort we are interested in developing methods for uncertainty propagation based on Polynomial Chaos expansions, which can be thought of as an extension of Volterra's theory of nonlinear functionals for stochastic systems [1]. Polynomial chaos (PC) was first introduced by Wiener [2] where Hermite polynomials were used to model stochastic processes with Gaussian random variables. According to Cameron and Martin [3] such an expansion converges in the  $\mathcal{L}_2$  sense for any arbitrary stochastic process with finite second moment. This applies to most physical systems. Xiu continuous and discrete distributions using orthogonal polynomials from the so called Askey-scheme [4] and demonstrated  $\mathcal{L}_2$  convergence in the correspond-

ing Hilbert functional space. This is popularly known as the generalized Polynomial Chaos (gPC) framework. The gPC framework has been applied to various applications including stochastic fluid dynamics [6], stochastic finite elements [7], and solid mechanics. Application of gPC to problems related to control and estimation of dynamical systems, has been surprisingly limited.

The work is organized as follows. We first present preliminaries on the theory of Polynomial Chaos and demonstrate transformation of stochastic dynamics, with parametric uncertainty, into deterministic dynamics in higher dimensional state space. We then present the stochastic Vinh's equation [9] for longitudinal motion where we assume uncertainty in ballistic coefficient, lift over drag ratio, density parameters and initial conditions. The stochastic hypersonic dynamics is then transformed into deterministic dynamics in higher dimensional state space using Polynomial Chaos expansions. This is followed by numerical results that characterize uncertainty propagation in state trajectories induced by uncertainty in system parameters. The results obtained from Polynomial Chaos framework are compared with Monte-Carlo simulations, which are shown to agree well.



## CHAPTER II

## POLYNOMIAL CHAOS

## A. Generalized Polynomial Chaos

Let  $(\Omega, \mathcal{F}, P)$  be a probability space, where  $\Omega$  is the sample space,  $\mathcal{F}$  is the  $\sigma$ -algebra of the subsets of  $\Omega$ , and  $P$  is the probability measure. Let  $\Delta(\omega) = (\Delta_1(\omega), \dots, \Delta_d(\omega)) : (\Omega, \mathcal{F}) \rightarrow (\mathfrak{R}^d, \mathcal{B}^d)$  be an  $\mathfrak{R}^d$ -valued continuous random variable, where  $d \in \mathfrak{N}$ , and  $\mathcal{B}^d$  is the  $\sigma$ -algebra of Borel subsets of  $\mathfrak{R}^d$ . A general second order process  $X(\omega) \in \mathcal{L}_2(\Omega, \mathcal{F}, P)$  can be expressed by Polynomial Chaos as

$$X(\omega) = \sum_{i=0}^{\infty} x_i \phi_i(\Delta(\omega)), \quad (2.1)$$

where  $\omega$  is the random event and  $\phi_i(\Delta(\omega))$  denotes the gPC basis of degree  $p$  in terms of the random variables  $\Delta(\omega)$ . The functions  $\{\phi_i\}$  are a family of orthogonal basis in  $\mathcal{L}_2(\Omega, \mathcal{F}, P)$  satisfying the relation

$$\mathbf{E}[\phi_i \phi_j] = \mathbf{E}[\phi_i^2] \delta_{ij}, \quad (2.2)$$

where  $\delta_{ij}$  is the Kronecker delta and  $\mathbf{E}[\cdot]$  denotes the expectation with respect to the probability measure  $dP(\omega) = f(\Delta(\omega))d\omega$  and probability density function  $f(\Delta(\omega))$ . Henceforth, we will use  $\Delta$  to represent  $\Delta(\omega)$ .

For random variables  $\Delta$  with certain distributions, the family of orthogonal basis functions  $\{\phi_i\}$  can be chosen in such a way that its weight function has the same form as the probability density function  $f(\Delta)$ . These orthogonal polynomials are members of the Askey-scheme of polynomials [4], which form a complete basis in the Hilbert space determined by their corresponding support. Table I summarizes the

correspondence between the choice of polynomials for a given distribution of  $\Delta$  [4].

Table I. Correspondence between choice of polynomials and given distribution of  $\Delta(\omega)$ .

Random Variable $\Delta$	$\phi_i(\Delta)$ of the Wiener-Askey Scheme
Gaussian	Hermite
Uniform	Legendre
Gamma	Laguerre
Beta	Jacobi

### B. Approximate Solution of Stochastic Differential Equations

A stochastic dynamical system of the form  $\dot{x} = f(x, \Delta)$ , where  $x \in \mathfrak{R}^n, \Delta \in \mathfrak{R}^d$ , can be solved using the Polynomial Chaos framework in the following manner. Assume solution of the stochastic differential equation to be  $x(t, \Delta)$ . For second order processes, the solution for every component of  $x \in \mathfrak{R}^n$  can be approximated as

$$\hat{x}_i(t, \Delta) = \sum_{j=0}^P x_{ij}(t) \phi_j(\Delta); \quad i = 1, \dots, n. \quad (2.3)$$

Substituting the approximate solution into the dynamical system results in error we get,

$$e_i = \dot{\hat{x}}_i - f_i(\hat{x}, \Delta); \quad i = 1, \dots, n.$$

The approximation in eqn.(2.3) is optimal in the  $\mathcal{L}_2$  sense when the projections of the error on the orthogonal basis functions are zero, i.e.,

$$\langle e_i(t, \Delta), \phi_j(\Delta) \rangle = \int_{\mathcal{D}_\Delta} e_i(t, \Delta) \phi_j(\Delta) f(\Delta) d\Delta = 0; \quad j = 0, \dots, P; \quad i = 1, \dots, n; \quad (2.4)$$

where  $\mathcal{D}_\Delta$  is the domain of  $\Delta$ . Equation, eqn.(2.4) results in  $n(P + 1)$  *deterministic* ordinary differential equations, which can be solved numerically to obtain the approximated stochastic response. Therefore, the stochastic dynamics in  $\mathfrak{R}^n$  has been transformed into deterministic dynamics in  $\mathfrak{R}^{n(P+1)}$ . The series is truncated after  $P + 1$  terms, which is determined by the dimension  $d$  of  $\Delta$  and the order  $r$  of the orthogonal polynomials  $\{\phi_j\}$ , satisfying  $P + 1 = \frac{(d+r)!}{d!r!}$ .

### C. Stochastic Dynamics and Polynomial Chaos

We first consider stochastic linear systems of the form

$$\dot{x}(t, \Delta) = A(\Delta)x(t, \Delta) + B(\Delta)u(t), \quad (2.5)$$

where  $x \in \mathfrak{R}^n$ ,  $u \in \mathfrak{R}^m$ . The system has probabilistic uncertainty in the system parameters, characterized by  $A(\Delta), B(\Delta)$ , which are matrix functions of random variable  $\Delta \equiv \Delta(\omega) \in \mathfrak{R}^d$  with certain *stationary* distributions. Due to the stochastic nature of  $(A, B)$ , the system trajectory will also be stochastic. The control  $u(t)$  is considered to be deterministic in this paper. We do not consider stochastic forcing in this paper, but this framework can be easily extended to include stochastic forcing and will be addressed in future publications.

Let us represent components of  $x(t, \Delta), A(\Delta)$  and  $B(\Delta)$  as,

$$x(t, \Delta) = [x_1(t, \Delta) \ \cdots \ x_n(t, \Delta)]^T, \quad (2.6)$$

$$A(\Delta) = \begin{bmatrix} A_{11}(\Delta) & \cdots & A_{1n}(\Delta) \\ \vdots & & \vdots \\ A_{n1}(\Delta) & \cdots & A_{nn}(\Delta) \end{bmatrix}, \quad (2.7)$$

$$B(\Delta) = \begin{bmatrix} B_{11}(\Delta) & \cdots & B_{1m}(\Delta) \\ \vdots & & \vdots \\ B_{n1}(\Delta) & \cdots & B_{nm}(\Delta) \end{bmatrix}. \quad (2.8)$$

By applying the Wiener-Askey gPC expansion to  $x_i(t, \Delta)$ ,  $A_{ij}(\Delta)$  and  $B_{ij}(\Delta)$ , we get

$$x_i(t, \Delta) = \sum_{k=0}^p x_{i,k}(t) \phi_k(\Delta) = \mathbf{x}_i(t)^T \Phi(\Delta), \quad (2.9)$$

$$A_{ij}(\Delta) = \sum_{k=0}^p a_{ij,k} \phi_k(\Delta) = \mathbf{a}_{ij}^T \Phi(\Delta), \quad (2.10)$$

$$B_{ij}(\Delta) = \sum_{k=0}^p b_{ij,k} \phi_k(\Delta) = \mathbf{b}_{ij}^T \Phi(\Delta), \quad (2.11)$$

where  $\mathbf{x}_i(t)$ ,  $\mathbf{a}_{ij}$ ,  $\mathbf{b}_{ij}$ ,  $\Phi(\Delta) \in \mathfrak{R}^p$  are defined by

$$\mathbf{x}_i(t) = [x_{i,0}(t) \cdots x_{i,p}(t)]^T, \quad (2.12)$$

$$\mathbf{a}_{ij} = [a_{ij,0}(t) \cdots a_{ij,p}(t)]^T, \quad (2.13)$$

$$\mathbf{b}_{ij} = [b_{ij,0}(t) \cdots b_{ij,p}(t)]^T, \quad (2.14)$$

$$\Phi(\Delta) = [\phi_0(\Delta) \cdots \phi_p(\Delta)]^T. \quad (2.15)$$

$$(2.16)$$

The number of terms  $p + 1$  is determined by the dimension  $d$  of  $\Delta$  and the order  $r$  of the orthogonal polynomials  $\{\phi_k\}$ , satisfying  $p + 1 = \frac{(d+r)!}{d!r!}$ . The coefficients  $a_{ij,k}$  and  $b_{ij,k}$  are obtained via Galerkin projection onto  $\{\phi_k\}_{k=0}^p$  given by

$$a_{ij,k} = \frac{\langle A_{ij}(\Delta), \phi_k(\Delta) \rangle}{\langle \phi_k(\Delta)^2 \rangle}, \quad (2.17)$$

$$b_{ij,k} = \frac{\langle B_{ij}(\Delta), \phi_k(\Delta) \rangle}{\langle \phi_k(\Delta)^2 \rangle}. \quad (2.18)$$

The  $n(p+1)$  time varying coefficients,  $\{x_{i,k}(t)\}; i = 1, \dots, n; k = 0, \dots, p$ , are obtained by substituting the approximated solution in the governing equation (eqn.(2.5)) and

conducting Galerkin projection onto  $\{\phi_k\}_{k=0}^p$ , to yield  $n(p+1)$  *deterministic* linear differential equations, given by

$$\dot{\mathbf{X}} = \mathbf{A}\mathbf{X} + \mathbf{B}u, \quad (2.19)$$

with  $\mathbf{X} \in \mathfrak{R}^{n(p+1)}$ ;  $\mathbf{M}, \mathbf{A} \in \mathfrak{R}^{n(p+1) \times n(p+1)}$ ;  $\mathbf{B} \in \mathfrak{R}^{n(p+1) \times m}$  and

$$\mathbf{X} = [\mathbf{x}_1^T \quad \mathbf{x}_2^T \quad \cdots \quad \mathbf{x}_n^T]^T, \quad (2.20)$$

$$\mathbf{A} = \mathbf{M}^{-1} \begin{bmatrix} \mathbf{A}_{11} & \cdots & \mathbf{A}_{1n} \\ \vdots & & \vdots \\ \mathbf{A}_{n1} & \cdots & \mathbf{A}_{nn} \end{bmatrix}$$

$$\mathbf{A}_{ij} = \langle \Phi \Phi^T \otimes \Phi^T \rangle (I_{p+1} \otimes \mathbf{a}_{ij}), \quad (2.21)$$

$$\mathbf{M} = I_n \otimes \begin{bmatrix} \langle \phi_0, \phi_0 \rangle & 0 & \cdots & 0 \\ 0 & \langle \phi_1, \phi_1 \rangle & \cdots & 0 \\ \vdots & \vdots & & \vdots \\ 0 & 0 & \cdots & \langle \phi_p, \phi_p \rangle \end{bmatrix},$$

$$\mathbf{B} = \begin{bmatrix} \mathbf{b}_{11} & \cdots & \mathbf{b}_{1m} \\ \vdots & & \vdots \\ \mathbf{b}_{n1} & \cdots & \mathbf{b}_{nm} \end{bmatrix},$$

where  $I_n \in \mathfrak{R}^{n \times n}$ ,  $I_{p+1} \in \mathfrak{R}^{(p+1) \times (p+1)}$  are identity matrices,  $\otimes$  is the Kronecker product, and the inner product in eqn.(2.21) is performed element wise. Therefore, transformation of a stochastic linear system with  $x \in \mathfrak{R}^n, u \in \mathfrak{R}^m$ , with  $p^{th}$  order gPC expansion, results in a *deterministic* linear system with increased dimensionality equal to  $n(p+1)$ .

Here we consider certain types of nonlinearities that may be present in the system model. The nonlinearities considered here are rational polynomials, transcendental functions and exponentials. We outline the process for representing these nonlinearities in terms of Polynomial Chaos expansions.

If  $x, y$  are random variables with gPC expansions similar to eqn.(2.9) then the gPC expansion of the expression  $xy$  can be written as

$$xy = \sum_{i=0}^p \sum_{j=0}^p x_i y_j \phi_i \phi_j.$$

The gPC expansion of  $x^2$  can be derived by setting  $y = x$  in the above expansion to obtain

$$x^2 = \sum_{i=0}^p \sum_{j=0}^p x_i x_j \phi_i \phi_j.$$

Similarly  $x^3$  can be expanded as

$$x^3 = \sum_{i=0}^p \sum_{j=0}^p \sum_{k=0}^p x_i x_j x_k \phi_i \phi_j \phi_k.$$

This approach can be used to derive the gPC expansions of any multi-variate whole rational monomial in general.

The gPC expansion of fractional rational monomials of random variables is illustrated using the the expression  $z = \frac{x}{y}$ . If  $x, y$  are random variables then  $z$  is also a random variable with gPC expansions similar to eqn.(2.9). The expansions of  $x, y$  are known. The gPC expansions of  $z$  can be determined using the following steps. Rewrite

$$z = \frac{x}{y} \text{ as } yz = x,$$

Expanding  $yz$  and  $x$  in terms of their gPC expansions gives

$$\sum_{i=0}^p \sum_{j=0}^p z_i y_j \phi_i \phi_j = \sum_{k=0}^p x_k \phi_k.$$

To determine the unknown  $z_i$  we project both sides of the equation on the subspace basis to obtain a system of  $p + 1$  linear equations

$$\frac{1}{\langle \phi_k, \phi_k \rangle} \sum_{i=0}^p \sum_{j=0}^p z_i y_j \langle \phi_i \phi_j \phi_k \rangle = x_k, \quad k = 0, \dots, p;$$

to solve for the  $p$  unknowns  $z_i$ . This can be generalized to obtain the gPC expansion of any fractional rational monomial.

When nonlinearities involve non polynomial functions, such as transcendental functions and exponentials, difficulties occur during computation of the projection on the gPC subspace. The corresponding integrals may not have closed form solutions. In such cases, the integrals either have to be numerically evaluated or these nonlinearities are first approximated as polynomials using Taylor series expansions and then the projections are computed using methods described above. While Taylor series approximation is straightforward and generally computationally cost effective, it can become severely inaccurate when higher order gPC expansions are required to represent the physical variability. A more robust algorithm is presented by Debusschere *et al.* [10] for any non polynomial function  $u(x)$  for which  $\frac{du}{dx}$  can be expressed as a rational function of  $x, u(x)$ .

#### D. Limitations of Polynomial Chaos

The gPC framework is well suited for evaluating short term statistics of dynamical systems. However, their performance degrades upon long term integration. Consider

the well known forced Van der Pol oscillator model,

$$\left. \begin{aligned} \dot{x}_1 &= x_2 \\ \dot{x}_2 &= -x_1 + \mu(\Delta)(1 - x_1^2)x_2 + u \end{aligned} \right\} \quad (2.22)$$

where  $\mu$  is a random variable with uniform distribution in the range  $\mu(\Delta) \in [0, 1]$ .

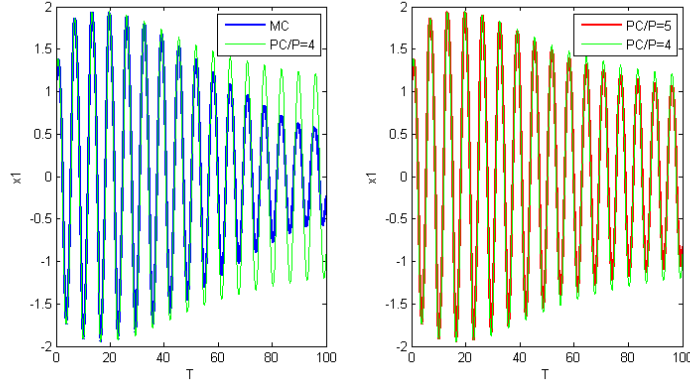


Fig. 4. Evolution of Monte Carlo(blue) and Polynomial Chaos(green and red) trajectories with time. With higher order of expansions Polynomial Chaos trajectory approaches the Monte Carlo trajectory.

As shown in fig. (4), the mean trajectories of the stochastic Van der Pol oscillator from eqn.(2.22), obtained from gPC calculations with 5<sup>th</sup> order expansions, deviate from those obtained from Monte-Carlo simulations. This deviation arises due to finite dimensional approximation of the probability space  $(\Omega, \mathcal{F}, P)$ . Several methods have been proposed to reduce this divergence, including adaptive [11] and multi-element approximation techniques [12]. We will include these approaches in our future work on trajectory generation with probabilistic uncertainty.



## CHAPTER III

VINH'S EQUATION WITH PROBABILISTIC UNCERTAINTY ON SYSTEM  
PARAMETERS

In this section we use Polynomial Chaos framework for analyzing uncertainty propagation in hypersonic flight vehicles. Here we consider 3DOF Vinh's equation to model hypersonic flight dynamics. Figure (5) shows a hypothetical model and the way the states are non dimensionalized.

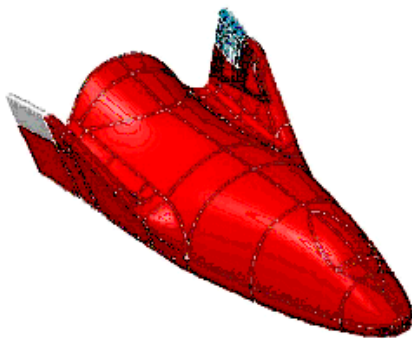


Fig. 5. Planar 3 dimensional Vinh's equation is used for modeling the dynamics. Here the states are height( $h$ ), velocity( $v$ ), flight path angle ( $\gamma$ ). The states( $h, v$ ) are non dimensionalized using the radius of the planet( $R_0$ ), and the escape velocity( $v_c$ )

The state variables are height  $h$  from surface of planet, velocity  $v$  and flight path angle  $\gamma$ . The equation of motion in the longitudinal plane is given by

$$\left. \begin{aligned} \dot{h} &= v \sin \gamma, \\ \dot{v} &= -\frac{\rho_0}{2B_c} \exp\left(\frac{h_2-hR_0}{h_1}\right)v^2 - \sin \gamma, \\ \dot{\gamma} &= \cos \gamma \left(\frac{v^2-1}{v}\right) + \frac{\rho_0\nu}{2B_c} \exp\left(\frac{h_2-hR_0}{h_1}\right)v, \end{aligned} \right\} \quad (3.1)$$

where  $R_0, h_1, h_2, B_c, \rho_0$  and  $\nu$  are constants as shown in table II.

Table II. Parameters for a Mars atmospheric entry vehicle.

Description	Symbol & Value
Density on the surface of Mars	$\rho_0 = 0.0176kg/m^3$
Gravitational Constant of Mars:	$\mu = 42.828 \times 10^3 Km/s^2$
Scale Height in Density Computation	$h_1 = 9.8 \times 10^3 m, h_2 = 20 \times 10^3 m$
Mean Equatorial radius of Mars	$R_0 = 3397Km$
Ballistic Coefficient	$B_c = 72.8kg/m^2$
Gravitational Oblateness Coeff. for Mars	$J_2 = 1960.45 \times 10^{-6}$
Lift to Drag Ratio	$\nu = 0.3$
Surface Gravity on Mars	$g_m = 3.71$

We consider uncertainty in parameters  $\rho_0$  (density on surface of Mars),  $\nu$  (lift over drag ratio) and  $B_c$  (ballistic coefficient). The uncertainty in these parameters are assumed to be uniform and we are interested in determining the uncertainty in state trajectories in flight and at the time when the vehicle strikes the ground.

When  $\nu, B_c$  and  $\rho_0$  are random variables, the differential equation defined by eqn.(3.1) is stochastic, and  $h, v$ , and  $\gamma$  are random processes. We use Polynomial Chaos framework to transform the stochastic differential equation into a deterministic differential equation in higher dimension state space. It is assumed that random variables  $\nu, B_c$  and  $\rho_0$  are expressed in terms of probability density functions. In this paper we assume uniform distribution on  $\nu, B_c$  and  $\rho_0$ . Therefore, from table(I), the basis functions are given by Legendre polynomials. The random variables  $\nu, B_c$  and  $\rho_0$  can then be written as,

$$\begin{aligned}
\nu(\Delta) &= \bar{\nu} + \delta\nu\Delta, \\
B_c(\Delta) &= \bar{B}_c + \delta B_c\Delta, \\
\rho_0(\Delta) &= \bar{\rho}_0 + \delta\rho_0\Delta,
\end{aligned}$$

where  $\Delta \in [-1, 1]$  and  $\delta\nu$ ,  $\delta B_c$ , and  $\delta\rho_0$  are the perturbations about nominal values  $\bar{\nu}$ ,  $\bar{B}_c$  and  $\bar{\rho}_0$  respectively. In this research we have assumed the parameters to have uniform distributions about their nominal values. The random processes  $h(t, \Delta)$ ,  $v(t, \Delta)$  and  $\gamma(t, \Delta)$  are expanded as

$$\begin{aligned}
h(t, \Delta) &= \sum_0^P h_i(t)\phi_i(\Delta), \\
v(t, \Delta) &= \sum_0^P v_i(t)\phi_i(\Delta), \\
\gamma(t, \Delta) &= \sum_0^P \gamma_i(t)\phi_i(\Delta).
\end{aligned}$$

Note that for the parameters with uniform uncertainty, only two basis functions are required to completely capture their respective probability density functions. No benefit is obtained by including more terms. However for the states, the expansion includes higher order basis functions. From the gPC theory, we are guaranteed exponential convergence as higher order basis functions are included[4].

Substituting these in eqn.(3.1) results in the following

$$\begin{aligned}
\sum_0^P \dot{h}_i\phi_i &= \sum_0^P v_i\phi_i \sin(\sum_0^P \gamma_i\phi_i), \\
\sum_0^P \dot{v}_i\phi_i &= -\frac{\rho_0(\Delta)}{2B_c(\Delta)} \left( \frac{\exp \frac{h_2}{h_1}}{\exp \frac{R_0 \sum_0^P h_i\phi_i}{h_1}} \right) \sum_0^P \sum_0^P \phi_i\phi_j v_i v_j - \sin(\sum_0^P \gamma_i\phi_i), \\
\sum_0^P \dot{\gamma}_i\phi_i &= \cos(\sum_0^P \gamma_i\phi_i) \left( \sum_0^P v_i\phi_i - \frac{1}{\sum_0^P v_i\phi_i} \right) + \frac{\rho_0(\Delta)\nu(\Delta)}{2B_c(\Delta)} \left( \frac{\exp \frac{h_2}{h_1}}{\exp \frac{R_0 \sum_0^P h_i\phi_i}{h_1}} \right) \sum_0^P v_i\phi_i.
\end{aligned}$$

The above equations are further simplified by the following substitutions

$$\begin{aligned}
\sum_0^P w_i \phi_i &= \frac{1}{\sum_0^P v_i \phi_i}, \\
\sum_0^P x_i \phi_i &= \frac{\exp \frac{h_2}{h_1}}{\exp \frac{R_0 \sum_0^P h_i \phi_i}{h_1}}, \\
\sum_0^P y_i \phi_i &= \frac{\rho_0(\Delta)}{2B_c(\Delta)}, \\
\sum_0^P z_i \phi_i &= \frac{\rho_0(\Delta)\nu(\Delta)}{2B_c(\Delta)},
\end{aligned}$$

where coefficients  $w_i, x_i, y_i, z_i \in \mathfrak{R}$  are yet to be determined. The Vinh's equation can now be written as

$$\begin{aligned}
\sum_0^P \dot{h}_i \phi_i &= \sum_0^P v_i \phi_i \sin \left( \sum_0^P \gamma_i \phi_i \right), \\
\sum_0^P \dot{v}_i \phi_i &= - \sum_{i,j,k,l=0}^P \phi_i \phi_j \phi_k \phi_l x_i y_j v_k v_l - \sin \left( \sum_{i=0}^P \gamma_i \phi_i \right), \\
\sum_0^P \dot{\gamma}_i \phi_i &= \cos \left( \sum_{i=0}^P \gamma_i \phi_i \right) \left( \sum_{i=0}^P v_i \phi_i - \sum_{i=0}^P w_i \phi_i \right) + \sum_{i,j,k=0}^P \phi_i \phi_j \phi_k x_i z_j v_k.
\end{aligned}$$

Taking Galerkin projection on basis functions  $\phi_i(\Delta)$ , we get the following deterministic differential equations,

$$\left. \begin{aligned}
\dot{h}_m &= \frac{1}{\langle \phi_m^2 \rangle} \sum_0^P v_i \langle \phi_i \phi_m \sin \left( \sum_0^P \gamma_i \phi_i \right) \rangle, \\
\dot{v}_m &= - \frac{1}{\langle \phi_m^2 \rangle} \sum_{i,j,k,l=0}^P \langle \phi_i \phi_j \phi_k \phi_l \phi_m \rangle x_i y_j v_k v_l - \frac{1}{\langle \phi_m^2 \rangle} \langle \phi_m \sin \left( \sum_{i=0}^P \gamma_i \phi_i \right) \rangle, \\
\dot{\gamma}_m &= \frac{1}{\langle \phi_m^2 \rangle} \sum_{i=0}^P v_i \langle \phi_i \phi_m \cos \left( \sum_{i=0}^P \gamma_i \phi_i \right) \rangle - \frac{1}{\langle \phi_m^2 \rangle} \sum_{i=0}^P w_i \langle \phi_i \phi_m \cos \left( \sum_{i=0}^P \gamma_i \phi_i \right) \rangle \\
&\quad + \frac{1}{\langle \phi_m^2 \rangle} \sum_{i,j,k=0}^P \langle \phi_i \phi_j \phi_k \phi_m \rangle x_i z_j v_k,
\end{aligned} \right\} \tag{3.2}$$

where  $m = 0, \dots, P$ . Equation (3.2) is the equivalent deterministic dynamics of the stochastic dynamics given by eqn.(3.1), approximated by gPC expansions. Solution

of this differential equation, in higher dimensional state space, can then be used to characterize  $h(t, \Delta)$ ,  $v(t, \Delta)$  and  $\gamma(t, \Delta)$ .

The terms  $w_i$ ,  $x_i$ ,  $y_i$  and  $z_i$  in eqn.(3.2) are computed as follows. Define

$$\alpha = \sum_0^P \gamma_i \phi_i, \quad \beta = \frac{R_0 \sum_0^P h_i \phi_i}{h_1}.$$

Multiplying,

$$\sum_0^P x_i \phi_i = \frac{\exp \frac{h_2}{h_1}}{\exp \frac{R_0 \sum_0^P h_i \phi_i}{h_1}},$$

by  $\exp(\beta)$  on both the sides we get

$$\exp \frac{h_2}{h_1} = \sum_0^P x_i \phi_i \exp \beta.$$

Taking projection on the basis functions yields,

$$\langle \exp \frac{h_2}{h_1} \phi_k \rangle = \langle \sum_0^P \phi_i \phi_k \exp \beta \rangle x_i.$$

This produces a set of  $(P + 1)$  linear equations in  $x_i$ . Similarly,  $w_i$  are computed by multiplying

$$\frac{1}{\sum_0^P v_i \phi_i} = \sum_0^P w_i \phi_i,$$

by  $\sum_0^P v_i \phi_i$  on both the sides, which reduces to

$$1 = \sum_0^P \sum_0^P \phi_i \phi_j v_i w_j.$$

Now taking projection on the basis functions we get,

$$\langle \phi_k \rangle = \sum_0^P \sum_0^P \langle \phi_i \phi_j \phi_k \rangle v_i w_j,$$

which also is a system of linear equations in  $w_i$ . The coefficients  $y_i$  and  $z_i$  can also be determined in the similar manner.

The terms  $\sin(\alpha)$  and  $\exp(\beta)$  are computed by approximating them by a Taylor series expansion of the perturbation about the mean [10]. For example, computing the exponential of a random variable  $\xi$ , the perturbation around the mean is given as  $d = \xi - \xi_0$ , where  $\xi_0$  is the mean. Therefore,

$$\exp(\xi) = \exp(\xi_0) \left( 1 + \sum_{n=1}^{N_{tay}} \frac{d^n}{n!} \right).$$

Here  $d$  is the stochastic part of  $\xi$  and  $N_{tay}$  is the number of terms in the Taylor series expansion. The sine of the random process is computed similar to the exponential, in the following manner,

$$\sin(\xi) = \sin(\xi_0 + d) = \sin(\xi_0) \cos(d) + \cos(\xi_0) \sin(d).$$

While Taylor series approximation is straightforward and generally computationally cost effective, it can become severely inaccurate when higher order gPC expansions are required to represent the physical variability.

#### A. Obtaining Statistics from Polynomial Chaos

Mean and variance of the state trajectories can be easily computed from the coefficients of the gPC expansions. The mean trajectories can be derived as,

$$\mathbf{E}[h(t, \Delta)] = \mathbf{E}\left[\sum_{i=0}^p h_i \phi_i\right] = \sum_{i=0}^p h_i \mathbf{E}[\phi_i] = \sum_{i=0}^p h_i \int_{\mathcal{D}_\Delta} \phi_i f d\Delta,$$

and similarly,

$$\mathbf{E}[v(t, \Delta)] = \sum_{i=0}^p v_i \int_{\mathcal{D}_\Delta} \phi_i f d\Delta,$$

$$\mathbf{E}[\gamma(t, \Delta)] = \sum_{i=0}^p \gamma_i \int_{\mathcal{D}_\Delta} \phi_i f d\Delta,$$

where  $h_i, v_i, \gamma_i$  are the coefficients of the gPC expansions of  $h(t, \Delta), v(t, \Delta), \gamma(t, \Delta)$  respectively, and  $f$  is the probability density function of the parameters.

The variance of a trajectory  $h(t, \Delta)$  is given by

$$\begin{aligned} \sigma^2[h(t, \Delta)] &= \mathbf{E}[(h(t, \Delta)^2) - \mathbf{E}[h(t, \Delta)]^2], \\ &= \sum_{i,j=0}^p h_i h_j \int_{\mathcal{D}_\Delta} \phi_i \phi_j f d\Delta - \mathbf{E}[h(t, \Delta)]^2 \\ &= \sum_{i=0}^p h_i^2 \int_{\mathcal{D}_\Delta} \phi_i^2 f d\Delta - \mathbf{E}[h(t, \Delta)]^2, \text{ because of orthogonality of } \phi_i, \phi_j. \end{aligned}$$

In this manner, the covariance matrix for the system can also be determined.

### 1. Uncertainty Propagation Using the Standard Approach of Monte Carlo Simulations

In the subsequent analysis, we have assumed 5% parametric variation in  $\rho_0, \nu$  and  $Bc$ , about the nominal values listed in table(II). The distribution is assumed to be uniform about the nominal values. We have obtained statistics of the states trajectories from Monte-Carlo simulations and have compared them with those obtained from Polynomial Chaos theory, to verify the validity of the Polynomial Chaos approach for analyzing uncertainty in hypersonic flight dynamics.

In the thesis work, we analyze the effect of uncertainty in initial condition and parameters on the downrange error and compare the results obtained from Monte-Carlo simulations and Polynomial Chaos theory. Numerical analysis is also performed to determine the sensitivity of the number of basis functions, Taylor series approximation and Debusschere's method, on the statistics of the state trajectories. In the simulation results shown, the dynamics has been non dimensionalized using the radius of planet and escape velocity.

Figures (6, 7 and 8) shows the results for uncertainty in initial conditions of  $h_0$ ,  $v_0$  and  $\gamma_0$  respectively. We observe that the state trajectories of the vehicle are greatly affected by the uncertainty in initial conditions and initial condition uncertainty is more when distribution is taken on  $v_0$ . These trajectories were obtained using Monte-Carlo simulations. Figures (9, 10 and 11) shows the evolution of uncertainty in state trajectories due to parametric uncertainty. We observe that the effect of uncertainty in  $\rho_0$ ,  $\nu$  and  $Bc$  are pronounced in lower altitudes where the aerodynamic effects are dominant. Also the uncertainty is more when it is taken for L over D ratio.

We next generate the mean trajectories of the system using Polynomial Chaos approach and the results agree with those obtained from Monte-Carlo simulations. Figures (12, 13 and 14 ) show the mean trajectories obtained from Monte-Carlo simulations and Polynomial Chaos theory, for uncertainty in parameters as initial conditions. We take 5% uniform uncertainty on each of the initial states( $h_0, v_0, \gamma_0$ ). The moments like mean and variance for the states is propagated and matched with the Monte Carlo simulation moments. We observe that Polynomial Chaos is able to capture the statistics of the state trajectories very well. The variance obtained by Polynomial Chaos is also matching with the Monte Carlo method.



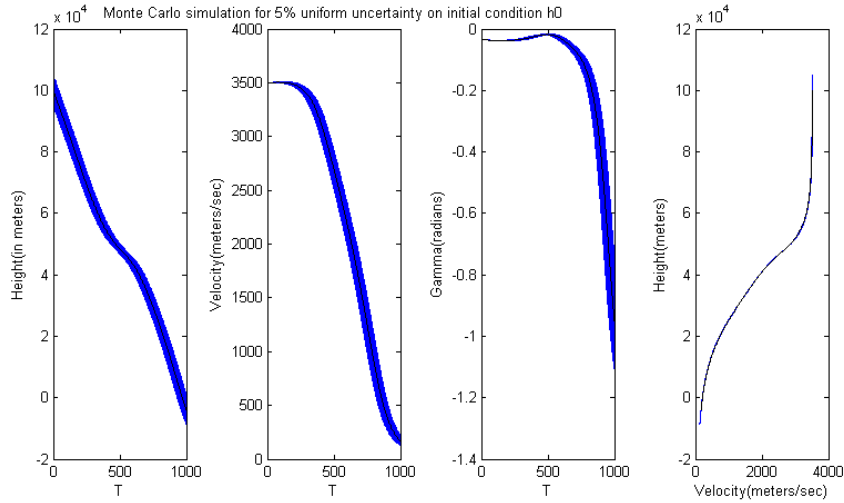


Fig. 6. Evolution of uncertainty using 5% uniform uncertainty on initial conditions of state  $h_0$ . The solid black trajectory is the mean trajectory.

## B. Simulation Results for the Moments Propagation Using Polynomial Chaos Theory

Moments are propagated using the Polynomial Chaos Theory. The results can be seen in figures (12, 13 and 14). Here the mean and the variance of the states are propagated using the Monte Carlo Simulation and again using the Polynomial Chaos Theory. We observe that the moments obtained from both the methods are matching. We are assuming 5% uniform uncertainty on the states  $(h_0, v_0, \gamma_0)$  as well as density  $(\rho_0)$ , ballistic constant  $(B_c)$  and L over D ratio  $(\nu)$ .

Figure (15) is for matching moments, between Monte Carlo and Polynomial Chaos Simulations, for uniform uncertainty in  $\rho_0$ . Figure(16) shows that by increasing the

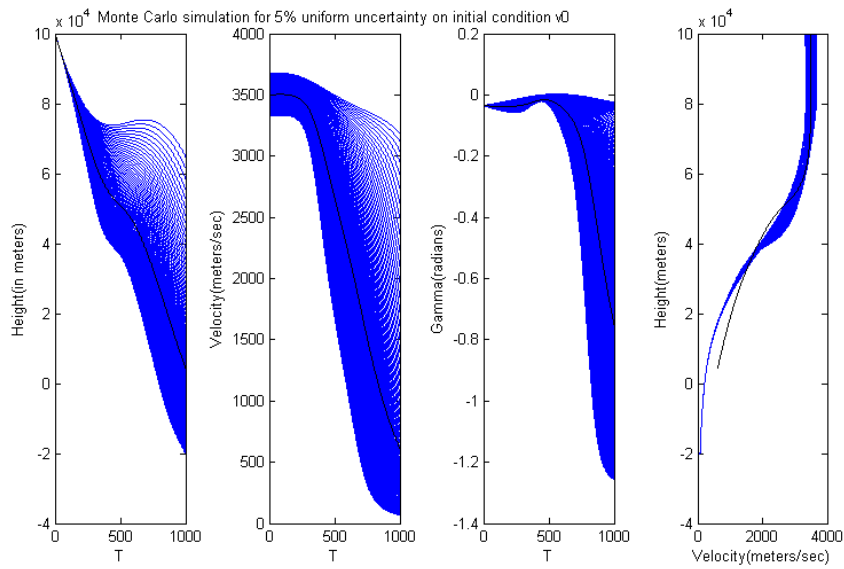


Fig. 7. Evolution of uncertainty using 5% uniform uncertainty on initial conditions of state  $v_0$ . Evolution of uncertainty is more predominant in this case. The solid black trajectory is the mean trajectory.

order of truncations the error between the Monte Carlo and the Polynomial Chaos Simulations converge.

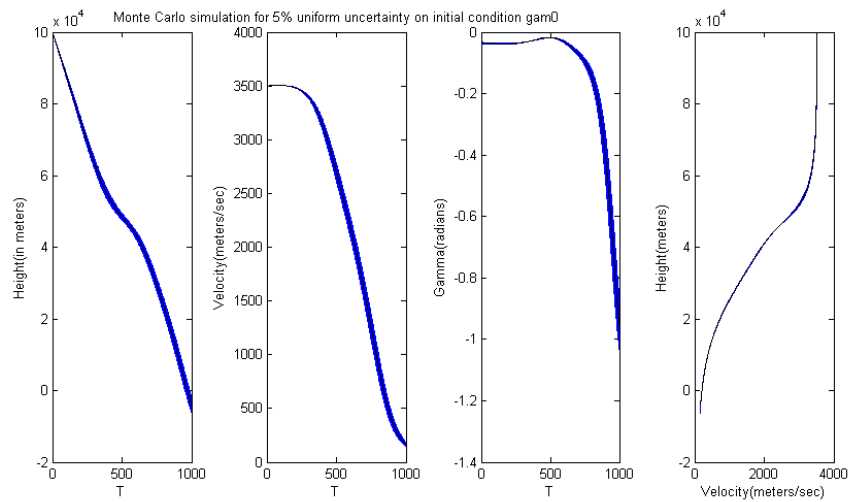


Fig. 8. Evolution of uncertainty using 5% uniform uncertainty on initial conditions of state  $\gamma_0$ . The solid black trajectory is the mean trajectory.

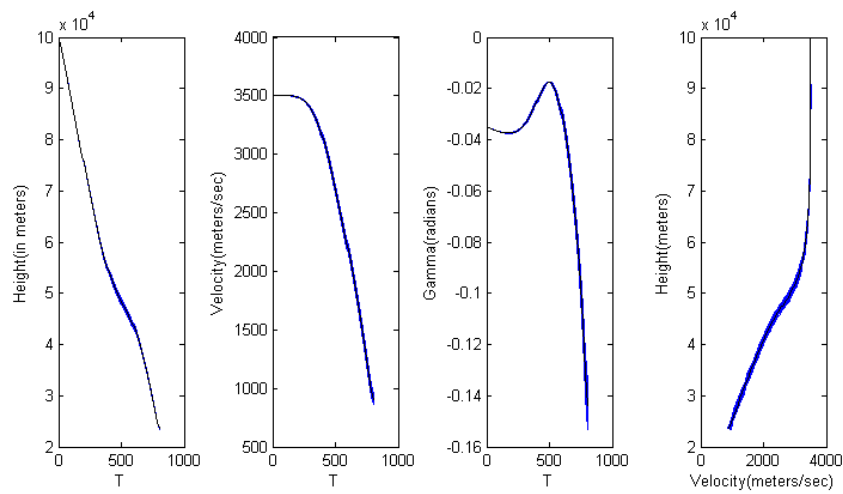


Fig. 9. Evolution of uncertainty using 5% uniform uncertainty on density ( $\rho_0$ ).

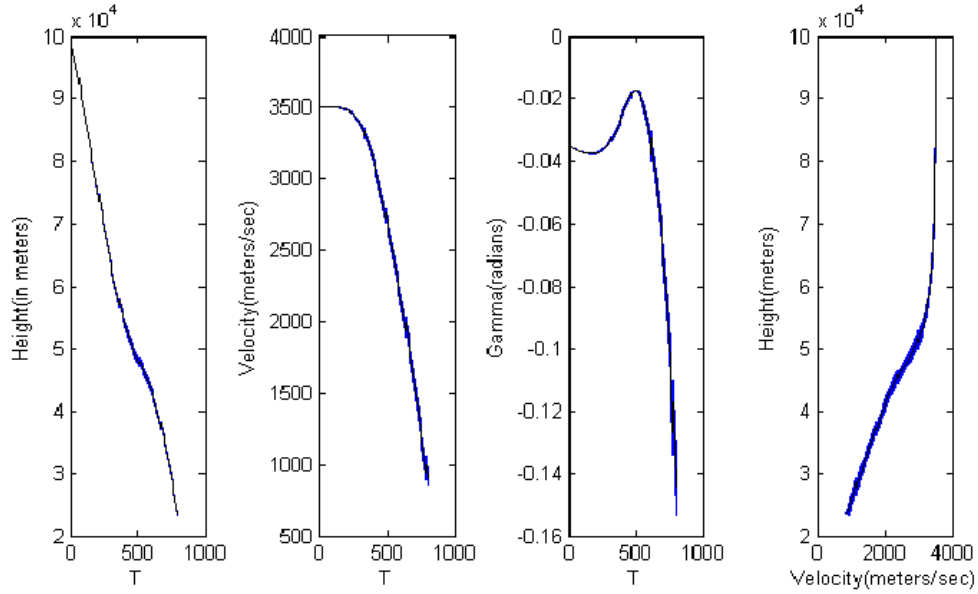


Fig. 10. Evolution of uncertainty using 5% uniform uncertainty on Ballistic Constant( $B_c$ ) ratio.

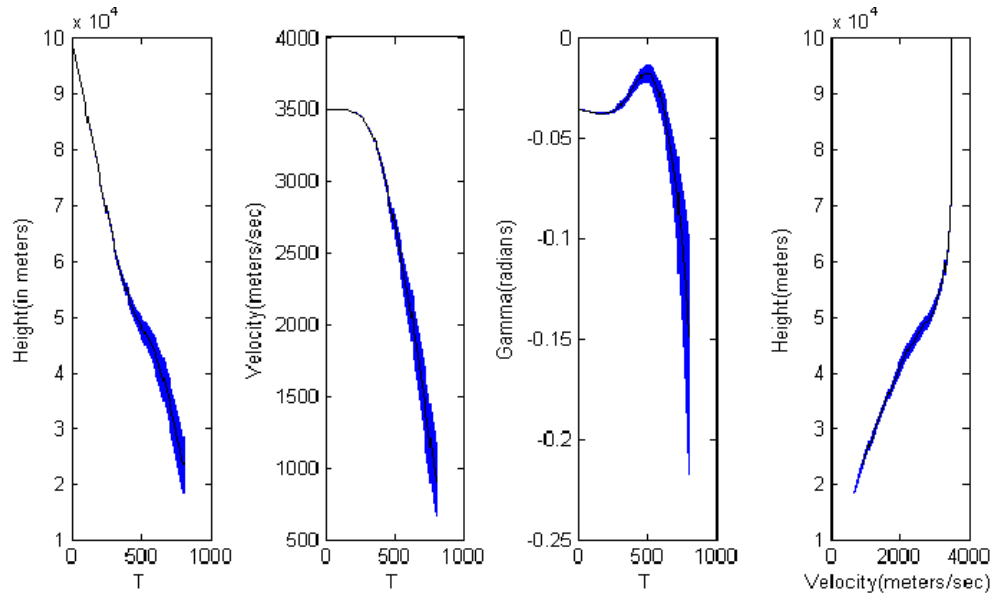


Fig. 11. Evolution of uncertainty using 5% uniform uncertainty on L over D ratio( $\nu_0$ ). We notice that the evolution of uncertainty is more in this case as compared to other parameters as  $B_c$  and  $\rho_0$ .

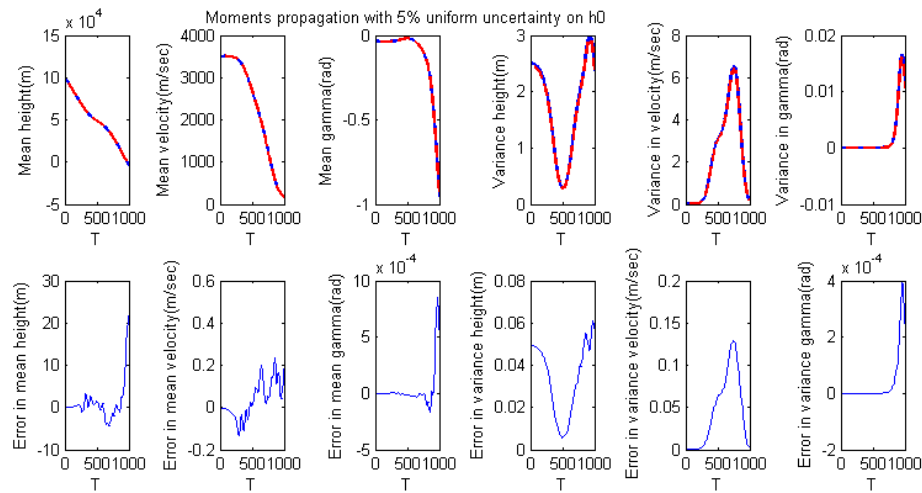


Fig. 12. Matching the moments, mean and variance, using 5% uniform uncertainty on  $h_0$  using the Sampling Method. Blue trajectory is from Monte Carlo method and red dashed is obtained from Polynomial Chaos method.

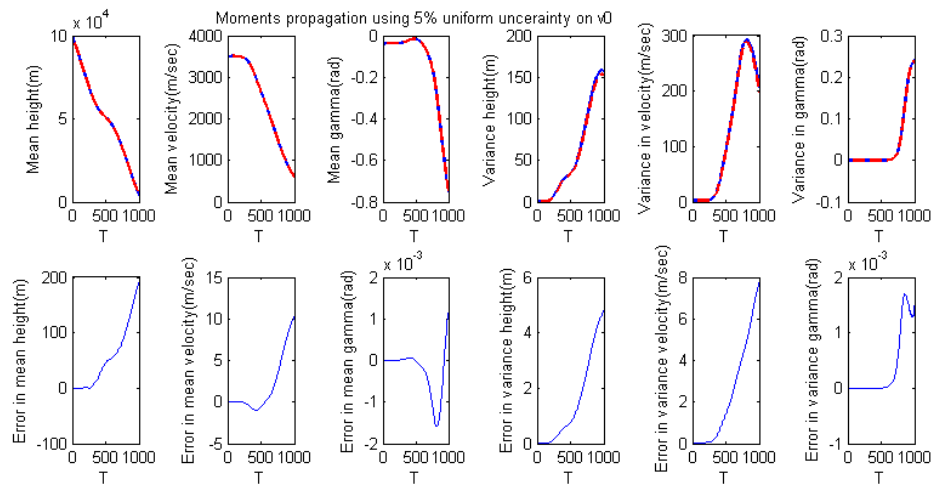


Fig. 13. Matching the moments, mean and variance, using 5% uniform uncertainty on  $v_0$  using the Sampling Method. Blue trajectory is from Monte Carlo method and red dashed is obtained from Polynomial Chaos method.

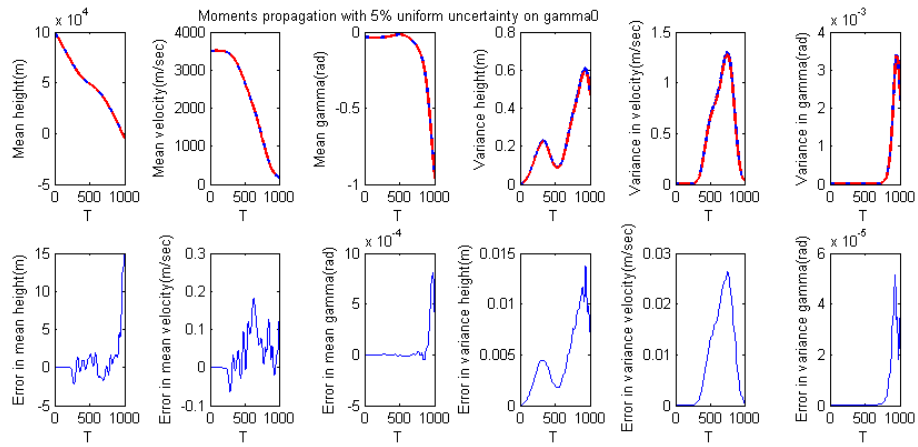


Fig. 14. Matching the moments, mean and variance, using 5% uniform uncertainty on  $\gamma_0$  using the Sampling Method. Blue trajectory is from Monte Carlo method and red dashed is obtained from Polynomial Chaos method.

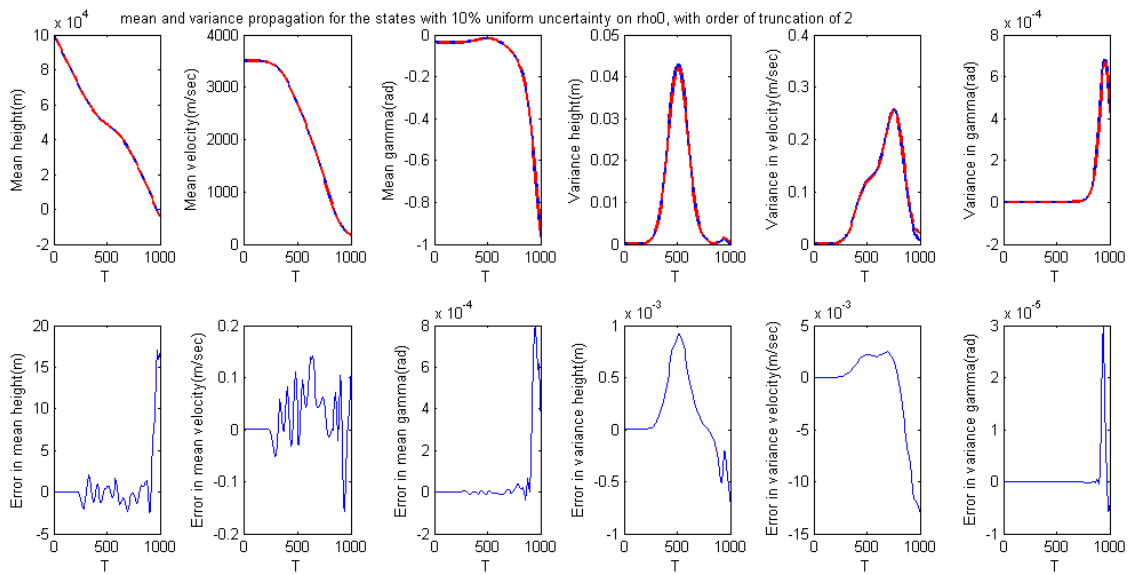


Fig. 15. Matching the moments, mean and variance, using 5% uniform uncertainty on  $\rho_0$  using the Sampling Method.

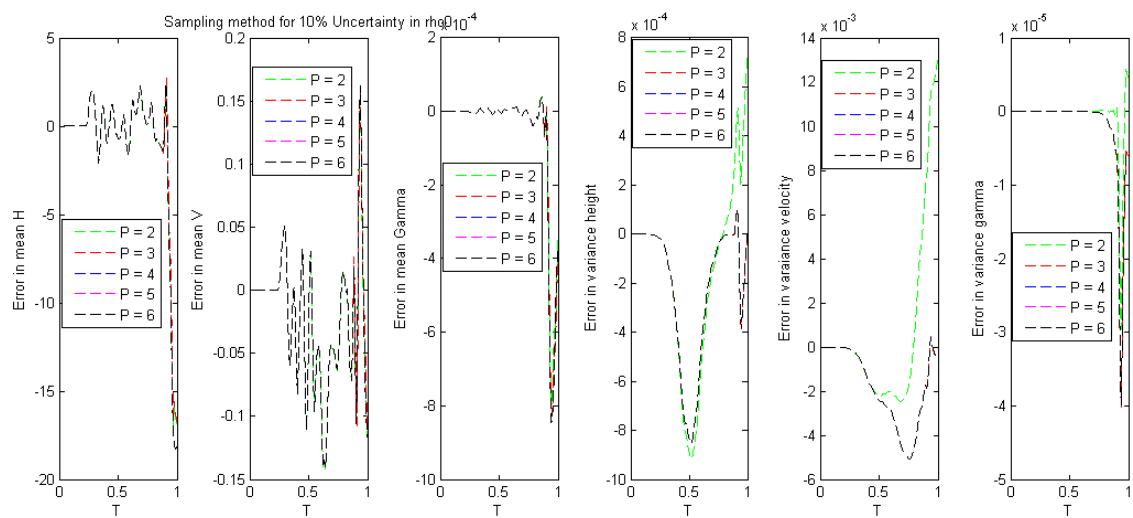


Fig. 16. Comparing the error in moments (mean and variance) using 5% uniform uncertainty on  $\rho_0$  and using the Sampling Method. Here the order of truncation is varied to see the convergence of the errors.

## CHAPTER IV

## CONTINUOUS LINEARIZATION APPROACH AND DOWNRANGE ANALYSIS

A variety of error sources contribute to the discrepancy between the position of the intended target and the position of the reentry vehicle. Though the sources have identifiable physical origin, it is not possible to assign the numerical value of precision to these uncertainties. However, it is feasible to establish a mean value of a given error source and a distribution of likely value that would closely resemble the uncertainty present on the parameters. To illustrate, the atmospheric property such as density or the parameters like ballistic constant or L by D ratio can be thought of having Gaussian distribution with a mean value and suitably chosen standard deviation about the mean. Let the nominal state or the state vector associated with the nominal trajectory be designated by  $\mathbf{X}_0$  and the actual state vector be  $\mathbf{X}$ . The error in the state vector can now be defined as

$$\mathbf{e} = \mathbf{X} - \mathbf{X}_0$$

A precise statistical description of the error state is given by the state covariance matrix  $P$ , defined as the expectation of all possible pairs of error vector components.

$$P = E[\mathbf{e}\mathbf{e}^T] = E[(\mathbf{X} - \mathbf{X}_0)(\mathbf{X} - \mathbf{X}_0)^T]$$

This gives us a powerful tool for assessing the size of the error vector and the degree of coupling among the components of the error vector. Hence, In assessing errors induced by uncertainty, a useful procedure is to define one trajectory - a nominal trajectory - assumed error free. The impact point of this trajectory is simply the intended impact point or the reference point. The remaining trajectories then become the perturbations, by some error source, about this nominal trajectory. We can then



separate the state vector  $\mathbf{X}$  into two parts. The nominal part  $\mathbf{X}_0$  and a perturbed part,  $\tilde{\mathbf{X}}$ , as

$$\mathbf{X} = \mathbf{X}_0 + \tilde{\mathbf{X}}$$

The nonlinear vector function can be linearized and written as follows:

$$\mathbf{F} \approx \mathbf{F}_0 + \frac{d\mathbf{F}}{d\mathbf{X}}(\mathbf{X} - \mathbf{X}_0)$$

Where a subscript 0 indicates the nominal trajectory. We insert the above equation to get

$$\frac{d\mathbf{X}_0}{dt} + \frac{d\tilde{\mathbf{X}}}{dt} \approx \mathbf{F}(\mathbf{X})|_{\mathbf{X}=\mathbf{X}_0} + \frac{d\mathbf{F}}{d\mathbf{X}}(\mathbf{X} - \mathbf{X}_0) = \mathbf{F}(\mathbf{X}_0) + \frac{d\mathbf{F}}{d\mathbf{X}}|_{\mathbf{X}_0}\tilde{\mathbf{X}}$$

But from the state equation we know:

$$\frac{d\mathbf{X}_0}{dt} = \mathbf{F}(\mathbf{X}_0)$$

Consequently,

$$\frac{d\tilde{\mathbf{X}}}{dt} = \frac{d\mathbf{F}}{d\mathbf{X}}|_{\mathbf{X}_0}\tilde{\mathbf{X}} = A\tilde{\mathbf{X}}$$

The above equation is the linear differential equation that describes perturbation about the nominal trajectory. The matrix A is the jacobian of the perturbational variables whose elements are given as follows

$$A = [a_{ij}] = \left[ \frac{\partial f_i}{\partial X_j} \right]_{\mathbf{X}=\mathbf{X}_0}$$

We note that the elements of matrix A is evaluated using the current states of the nominal trajectory. Even though the elements of A are time varying, reflecting the time varying states of the nominal trajectory, the elements of A are treated as time constant for integration of the perturbational variable  $\tilde{\mathbf{X}}$ . A convenient way of representing the relationship between the perturbational state vector  $\tilde{\mathbf{X}}$  at time  $t_i$  and

time  $t_{i+1}$  is by the use of the transition matrix,  $\phi$ . Hence

$$\tilde{\mathbf{X}}_{i+1} = \phi(t_{i+1}, t_i)\tilde{\mathbf{X}}_i$$

If  $\phi$  is assigned some fixed value by the nominal states, then according to the above equation,  $\phi$  may be accepted as a matrix that transitions the perturbation or the error state vector  $\tilde{\mathbf{X}}$  over the time interval  $t_i$  to  $t_{i+1}$ . The transition matrix  $\phi$  can formally be identified with the matrix exponent and more usefully with the matrix series.

$$\phi(t_{i+1}, t_i) = e^{A(t_{i+1}-t_i)} = e^{A\Delta t}$$

Which can conveniently be expanded as

$$\phi = I + A\Delta t + \frac{1}{2!}A^2\Delta t^2 + \frac{1}{3!}A^3\Delta t^3 + \dots + \frac{1}{n!}A^n\Delta t^n$$

Further we note that the error ellipsoid is the quadratic form of the covariance matrix.

We define the error covariance matrix at time  $t_i$ ,  $P_i$  as

$$P_i = E[\tilde{\mathbf{X}}_i\tilde{\mathbf{X}}_i^T]$$

Where  $\tilde{\mathbf{X}}_i$  is the perturbational or error state vector at time  $t_i$ . It can now be inferred for time  $t_{i+1}$  that

$$P_{i+1} = E[\tilde{\mathbf{X}}_{i+1}\tilde{\mathbf{X}}_{i+1}^T]$$

Hence insertion of equation gives:

$$P_{i+1} = \phi_i P_i \phi_i^T$$

The preceding equation provides the discrete propagation of the covariance matrix. Using the expansion of the state transition matrix we get

$$P_{i+1} \approx [(I + A\Delta t)P_i(I + A\Delta t)^T]$$

Which upon simplification gives

$$\frac{P_{i+1} - P_i}{\Delta t} = AP_i + P_iA^T$$

We use the above approach for computing the covariance matrix. The nominal trajectory is computed assuming that the parameters are known with certainty and the jacobian of the perturbational variables are computed about the nominal trajectory. This approach is used for populating the covariance matrix along the nominal trajectory.

#### A. Simulation Results

Here the simulation is run with Gaussian distribution on the parameters and the three methods, Monte Carlo, Polynomial Chaos and Continuous Linearization approach is compared.

#### B. State Acquisition

It is common to use the estimation or optimization algorithms for the system whose states are given by the equation of the form:

$$\dot{\mathbf{x}} = \mathbf{f}(t, \mathbf{x}, \mathbf{p})$$

Where,

$$\mathbf{p} = [p_1, p_2, p_3, \dots, p_q]^T$$

is a set of model constants which appear in the system's differential equations. In our application initial conditions are poorly known as well as one or more elements of the model parameters vector  $\mathbf{p}$ . Hence it becomes necessary to estimate both  $\mathbf{x}(t_0)$  and  $\mathbf{p}$  based upon the measurements of  $\mathbf{x}(t)$  or a function thereof. Conventional estimation require the partial derivative matrices:

$$\Phi(t, t_0) = \frac{\partial \mathbf{x}(t)}{\partial \mathbf{x}(t_0)}$$

and,

$$\Psi(t, t_0) = \frac{\partial \mathbf{x}(t)}{\partial \mathbf{p}}$$

These derivative matrices can be computed as

$$\mathbf{x}(t) = \mathbf{x}(t_0) + \int_{t_0}^t \mathbf{f}(\tau, \mathbf{x}, \mathbf{p}) d\tau$$

This when applied to the derivative matrices give:

$$\Phi(t, t_0) = I + \int_{t_0}^t \frac{\partial \mathbf{f}(\tau, \mathbf{x}, \mathbf{p})}{\partial \mathbf{x}(\tau)} \frac{\partial \mathbf{x}(\tau)}{\partial \mathbf{x}(t_0)} d\tau$$

and

$$\Psi(t, t_0) = \int_{t_0}^t \left( \frac{\partial \mathbf{f}(\tau, \mathbf{x}, \mathbf{p})}{\partial \mathbf{p}} + \frac{\partial \mathbf{f}(\tau, \mathbf{x}, \mathbf{p})}{\partial \mathbf{x}(\tau)} \frac{\partial \mathbf{x}(\tau)}{\partial \mathbf{x}(t_0)} \right) d\tau$$

Taking the time derivative of the above equations we see that the desired derivative matrices satisfy the first order linear differential equations:

$$\dot{\Phi}(t, t_0) = F(t)\Phi(t, t_0)$$

Where  $\Phi(t_0, t_0) = I$ , and

$$\dot{\Psi}(t, t_0) = F(t)\Psi(t, t_0) + \frac{\partial \mathbf{f}(t, \mathbf{x}, \mathbf{p})}{\partial \mathbf{p}}$$

with  $\Psi(t_0, t_0) = 0$  and

$$F(t) = \frac{\partial f(t, \mathbf{x}, \mathbf{p})}{\partial x(t)}$$

The above derivations can be viewed in a more systematic way by augmenting the system differential equation as:

$$\dot{\mathbf{x}} = \mathbf{f}(t, \mathbf{x}, \mathbf{p})$$

$$\dot{\mathbf{p}} = 0$$

The above equations can be rewritten as

$$\dot{\mathbf{z}} = \mathbf{g}(t, \mathbf{z})$$

Where,  $\mathbf{z} \equiv [\mathbf{x}^T \mathbf{p}^T]^T$  and  $\mathbf{g}(t, \mathbf{z}) \equiv [\mathbf{f}^T \mathbf{0}^T]^T$ . We now form this augmented matrix:

$$\Gamma(t, t_0) \equiv \frac{\partial \mathbf{z}(t)}{\partial \mathbf{z}(t_0)} = \begin{bmatrix} \Phi(t, t_0) & \Psi(t, t_0) \\ 0 & I \end{bmatrix} \quad (4.1)$$

$$(4.2)$$

The augmented state transition matrix satisfies:

$$\dot{\Gamma}(t, t_0) = \frac{\partial \mathbf{g}(t, \mathbf{z})}{\partial \mathbf{z}(t)} \Gamma(t, t_0)$$

and

$$\Gamma(t, t_0) = I$$

Where,

$$\frac{\partial \mathbf{g}(t, \mathbf{z})}{\partial \mathbf{z}(t)} = \begin{bmatrix} F(t) & \frac{\partial(t, \mathbf{x}, \mathbf{p})}{\partial \mathbf{p}} \\ 0 & 0 \end{bmatrix} \quad (4.3)$$

$$(4.4)$$

The augmented state transition matrix is now used to obtain the statistics when the initial condition is poorly known and uncertainty is present on one of the parameters. In our simulation we assume that uncertainty is present on the initial condition as well as on one of the parameters  $\rho_0$ ,  $\nu$  or  $B_c$  in the form of Gaussian distribution. The simulation is done for each of the three methods, Monte Carlo, Polynomial Chaos and Continuous Linearization and statistics is obtained in the form of mean and variances of the state trajectories.

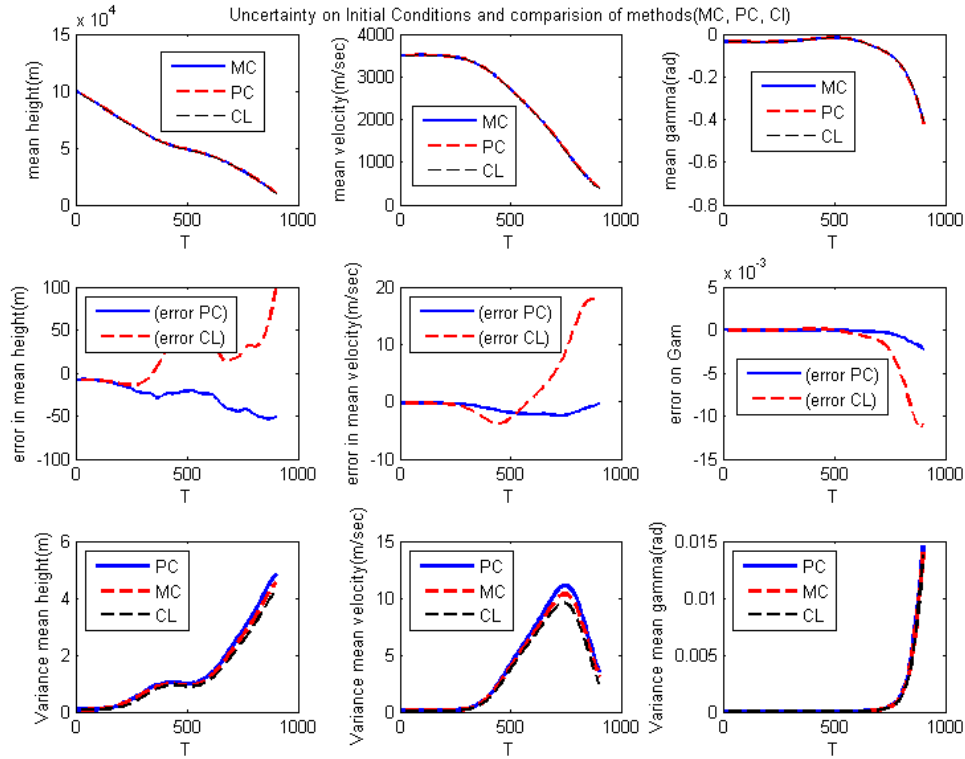


Fig. 17. Matching the moments, mean and variance, using 5% Gaussian uncertainty on IC for the three approaches (MC, PC, CL).

Next, we analyze the continuous linearization approach to obtain the statistics for the states of the Vinh's equation. We are considering the enhanced state dynamics

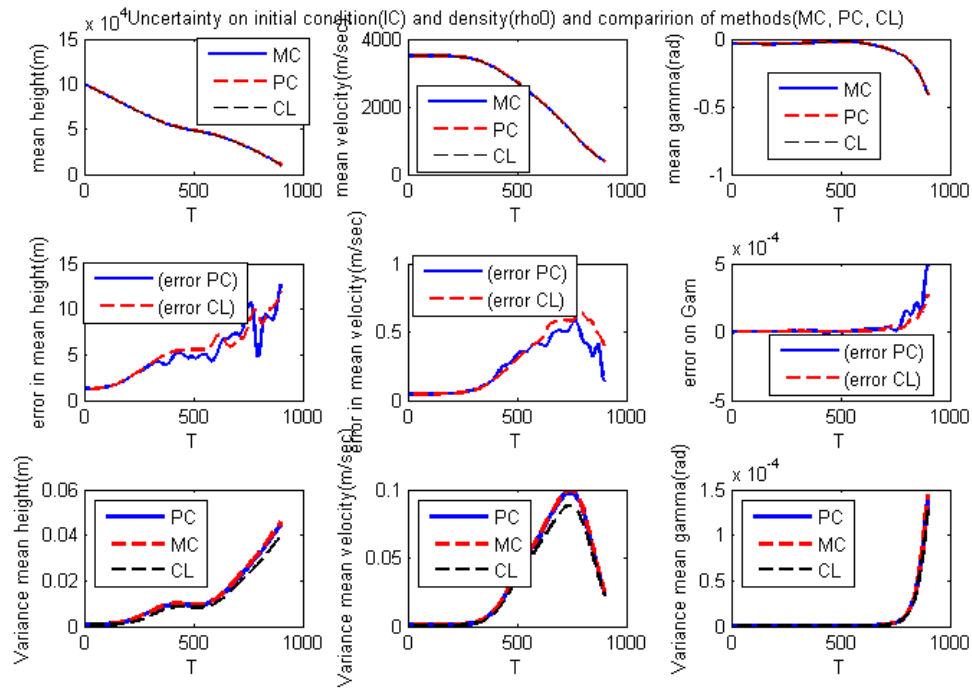


Fig. 18. Matching the moments, mean and variance, using 5% Gaussian uncertainty on IC and  $\rho_0$  for the three approaches (MC, PC, CL).

to account for the Gaussian Uncertainty in one of the parameters ( $\rho_0$ ,  $B_c$ ,  $\nu$ ) together with uncertain initial conditions. The method to obtain the mean and the variance trajectories has already been explained in previous chapter. For a given Monte Carlo trajectory the Gaussian random number generator is entered with the appropriate standard deviation and the trajectories are generated for uncertain initial condition and one of the parameters. The random numbers used in the Monte Carlo process are then combined to form an error covariance matrix by correlating each state taken two at a time. The resulting matrix so formed at the start of the Monte Carlo simulation is used to initialize the covariance propagation procedure that is terminated at the time of nominal trajectory impact. We note immediately that the three state trajectories for the moments of the random variables ( $h$ ,  $v$ ,  $\gamma$ ) obtained each for the

Monte Carlo, Polynomial Chaos and Continuous Linearization approach agree well. The simulation is first done for Gaussian uncertainty in Initial conditions on states, Figure (17). We observe that Polynomial Chaos is more accurate as compared to Continuous Linearization approach and the errors, when the trajectories are compared with the standard Monte Carlo trajectory, is smaller in the case of Polynomial Chaos. We see that is true for second order moments too. The Polynomial Chaos approach works reasonably well over the Continuous Linearization approach when the uncertainty on Initial conditions are taken. Figure(18) shows the result where it is seen that Polynomial Chaos gives relatively far better result than Continuous Linearization Approach . We extend the effort by taking the combined uncertainty on the Initial Condition and density as well. We consider 5% Gaussian Uncertainty on initial condition and density simultaneously. Figures (18, 19, 20) illustrates the result. The first one of them shows the mean trajectories being compared for Monte Carlo, Polynomial Chaos and the Continuous Linearization approach. This is done by taking Gaussian uncertainty on the parameters initial conditions combined with density  $\rho_0$  and subsequently with  $B_c$  and L over D ratio( $\nu$ ). We next set to compare the variances obtained by the three approaches. They also match well but we note that Polynomial Chaos approach is giving better results than Continuous Linearization approach when the trajectories are compared with Monte Carlo Simulations.



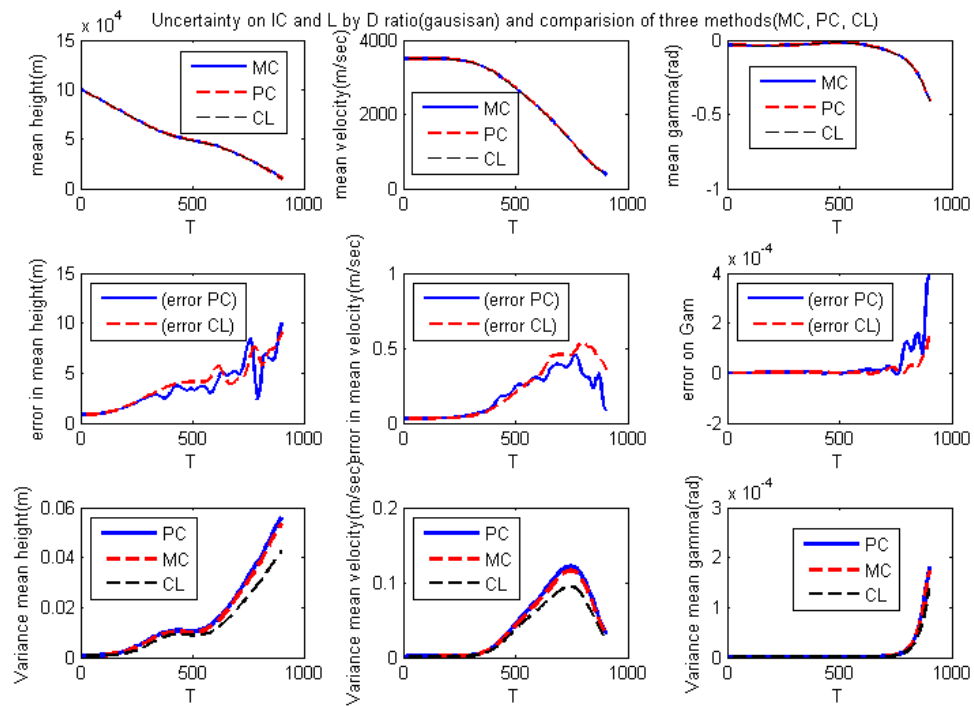


Fig. 19. Matching the moments, mean and variance, using 5% Gaussian uncertainty on IC and L over  $D(\nu)$  ratio for the three approaches (MC, PC, CL).

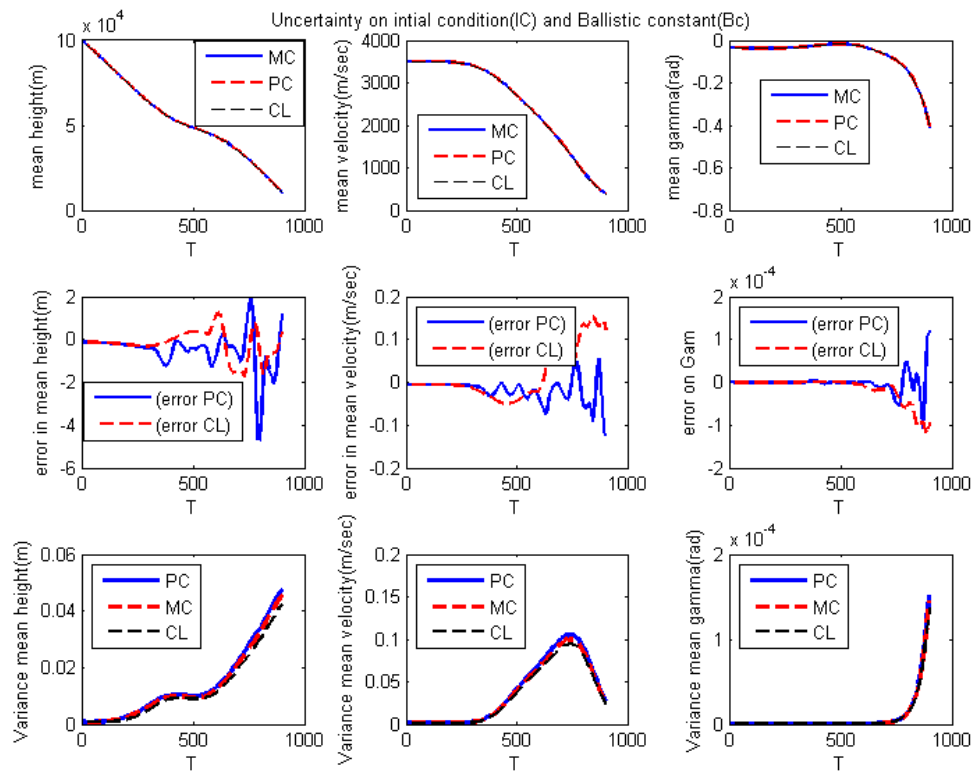


Fig. 20. Matching the moments, mean and variance, using 5% Gaussian uncertainty on IC and Bc ratio for the three approaches (MC, PC, CL).

## CHAPTER V

## SUMMARY AND CONCLUSIONS

## A. Summary

In this thesis, we have presented a framework for analyzing evolution of uncertainty in hypersonic flight. This framework is based on the generalized Polynomial Chaos framework, which has been successfully applied to areas such as stochastic computational fluid dynamics and solid mechanics. We have demonstrated that this framework captures the trajectory statistics quite accurately and is computationally less demanding than methods based on Monte-Carlo simulations. Monte-Carlo methods were used in this paper solely to verify the results obtained from the generalized Polynomial Chaos approach.

However, the generalized Polynomial Chaos based approach has limitations related to errors due to long term integration. This makes it suitable for estimation of short term statistics. Further, we have used this method to capture the dynamics with fewer dimensions. Further, in terms of computation, Polynomial Chaos requires some effort in computing the tensors  $\langle \phi_i \phi_j \cdots \phi_l \rangle$ , which has to be done once. This can be computed in the preprocessing stage and stored for later use. It is the computation of these tensors that makes higher order Taylor series approximation computationally prohibitive. In general Polynomial Chaos based approach is computationally far superior to Monte-Carlo methods.

## B. Future Work

Polynomial Chaos has long term integration issues. It cannot capture the statistics of the dynamics over a long period of time. This was demonstrated for the well known Van der Pol dynamics where the trajectory obtained by the Polynomial Chaos deviated from the Monte Carlo trajectories. This will become more apparent when the stochastic solutions are periodic with frequencies varying in random fashion. We can choose the polynomial order adaptively but it will increase the computational burden. Methods exist that reduce the error growth over time and they incorporate adaptive multi-element schemes [11, 12]. The multi-element approach approximates  $\Omega$  using local approximations, instead of global approximations. It is well known in approximation theory that locally supported basis functions provide superior results than globally supported functions. The idea works on the framework of Multi-Element generalized Polynomial Chaos where the random space is decomposed into smaller elements and the gPC scheme is implemented for each of the elements. This will allow us to work with low polynomial order as even the lower order approximation will capture the short term statistics. This multi element gPC method is analogous to h-p type convergence in Finite Element Theory. Here h will be the size of the random element and p will be the order of the Polynomial Chaos.

We have used this method when the forcing is not there. For most of the practical cases we have forcing of stochastic nature. Polynomial Chaos scheme can be used in this case if the forcing is represented using Karhunen-Loeve expansions. This is the representation of the stochastic process as an infinite linear combination of orthogonal basis functions. The choice of basis functions is not restricted. The particular interest is to restrict the basis functions to those which will make  $X_i$  uncorrelated

random variables. Mathematically this will require:

$$E[X_i X_j] = E[X_i]E[X_j]$$

$$\forall i, j \neq i$$

gPC works for standard distributions like uniform, Gaussian. Since most of the practical simulations involve non standard type distributions, this method should be extended to capture the dynamics with non standard distributions. This is done by choosing the set of orthogonal polynomials using Gram-Schmidt orthogonalization. Mathematically, the orthogonal polynomials can be represented as:

$$\phi_j(\xi) = e_j(\xi) - \sum_{k=0}^{j-1} c_{jk} \phi_k(\xi)$$

with  $\phi_0 = 1$  and

$$c_{jk} = \frac{\langle e_j(\xi), \phi_k(\xi) \rangle}{\langle \phi_k(\xi), \phi_k(\xi) \rangle}$$

Here the polynomials  $e_j(\xi)$  are polynomials of exact degree  $j$ . Further, to obtain exponential convergence the weighting function has to be equal to the probability distribution function(PDF) of the random variable. This will extend the use of gPC method to other non standard type of distributions as well with exponential convergence realized.

Although we have shown that the gPC scheme works well over the standard Monte Carlo method for three dimensional stochastic planar dynamics, it needs to be checked as how will this behave with cases having multi dimensional random spaces. It is apparent that the evaluation of statistics of the dynamics will become more involved. This approach might have problems when applied to partial differential equations

with random fields.

## REFERENCES

- [1] V. Volterra., *Lecons sur les Equations Integrales et Integrodifferentielles*. Paris: Gauthier Villars, 1913.
- [2] N. Weiner., “The homogeneous chaos,” *AJM*, vol. 60, no. 4, pp. 897-936, 1938.
- [3] R. H. Cameron and W. T. Martin., “The orthogonal developpment of non-linear functionals in series of Fourier-Hermite Functionals,” *Ann Math*, vol. 48, no. 2, pp. 385-392, 1947.
- [4] D. Xiu and G. Em Karniadakis., “The Weiner Askey Polynomial Chaos for stochastic differential equations ,” *SIAM J. Sci. Comput.*, vol. 24, no. 2, pp. 619-644, 2002.
- [5] R. Askey and J. Wilson., “Some basic hypergeometric polynomials that generalize Jacobi Polynomials,” *Memoirs Amer. Math. Soc.*, vol. 66, no. 7, pp. 319-360, 1985.
- [6] T. Y. Hou, W. Luo, B. Rozovskii, and Hao-Min Zhou. “Weiner Chaos Expansions and numerical solutions of randomly forced equations of fluid mechanics.,” *J. Comput. Phys.*, vol. 187, no. 1, pp. 137-167, 2003.
- [7] R. G. Ghanem and Pol D. Spanos, *Stochastic Finite Elements: A Spectral Approach*. New York: Springer-Verlag, 1991.
- [8] R. Ghanem and J. Red-Horse., “Propagation of probabilistic uncertainty in complex physical systems using a stochastic finite element approach,” *Phys. D.*, vol. 133, nos. 1-4, pp. 137-144, 1999.

- [9] N. Vinh. *Hypersonic and Planetary Entry Flight Mechanics.*, Ann Arbor, MI: University of Michigan Press, June 1980.
- [10] B. J. Debusschere, H. N.Najm, P. P. Pebay, Omar M. Knio, R. G. Ghanem and O. P. Le Maitre. “Numerical challenges in the use of Polynomial Chaos representations for stochastic processes,” *SIAM J. Sci. Comput.*, vol. 26 no. 2, pp. 698-719, 2005.
- [11] R. Li and R. Ghanem. “Adaptive Polynomial Chaos expansions applied to statistics of extremes in non linear random vibration.,” *Probabilist Eng Mech*, vo. 13, pp 125-136, April 1998.
- [12] X. Wan and G. Em Karniadakis., “An adaptive multi-element generalized Polynomial Chaos method for stochastic differential equations.,” *J. Comput. Phy.*, vol. 209, no. 2, pp. 617-642, 2005.
- [13] S. I. Resnick, *A Probability Path.*, Boston, MA: Birkhäuser, 1998.
- [14] M. Jardak, C.-H. Su, G.E. Karniadakis. “Spectral polynomial choas solutions of the stochastic advection equation.,” *J. Sci Comput.*, vol. 17, pp. 319- 338, 2002.
- [15] G. Lin, C.-H. Su, G.E. Karniadakis, “Stochastic solvers for the euler equations,” *43rd AIAA Aerospace Sciences Meeting and exhibit* Reno, Nevada, 2005.
- [16] L. Mathelin, M.Y. Hussaini, T. Z. Zang., “Stochastic approches to uncertainty quantification in CFD simulations,” *Numerical Algorithms*, vol. 38, pp. 209 - 236, 2005.



## APPENDIX A

## NOMENCLATURE

$\Omega$	Sample space
$\mathcal{F}$	$\sigma$ -algebra defined over subsets of $\Omega$
$P$	Probability measure
$\omega \in \Omega$	An event in the sample space
$\Delta \equiv \Delta(\omega)$	Random variables representing system parameters
$f(\Delta)$	Joint probability density function of system parameters
$h$	Non dimensional altitude, scaled by $R_0$
$V$	Non dimensional velocity, scaled by $v_c$
$\gamma$	Flight path angle
$L/D$	Lift over drag ratio
$B_c$	Ballistic coefficient of vehicle
$\rho_0$	Density on surface of planet
$t$	Non dimensional time, scaled by $R_0/v_c$
$g$	$GM/R_0^2$
$R_0$	Radius of planet
$v_c$	Escape velocity = $\sqrt{gR_0}$
$M$	Mass of planet
$G$	Universal gravitation constant

## APPENDIX B

## DIFFERENT METHODS FOR UNCERTAINTY PROPAGATION

Monte Carlo methods belong to a class of computational algorithms which uses repeated random sampling for the computation. This becomes computationally cost prohibitive as the number of sample points increase as the mathematical or physical simulation needs to be run for each of the sample points. This technique is often used when deterministic algorithm is not present to compute the exact result. This method is particularly helpful in analyzing a system with large number of coupled degrees of freedom such as fluids, disordered materials or strongly coupled solids. It is used for modeling phenomena with significant uncertainty in inputs or parameter constants. The general pattern for using this approach is to select a domain with random possible inputs. This domain is used for generating random inputs and performing a deterministic computation on them. The results of individual computation is collected to get the final result. As an illustrative example, this method can be used for the evaluation of definite integrals with complicated boundary conditions which cannot be defined analytically or as in our case it is used for computing the statistics like mean and variance of the states defined by the dynamical differential equation where it is realized for each of the sample points in the domain selected for the parameters like initial condition and constants.

Consider the differential equation:

$$dX = f(x)dt + dW$$

Replacing the non linear system by the equivalent linear system:

$$\dot{\bar{X}}_{eq} = (A(t)\bar{X}_{eq} + b(t))dt + dW$$

Now, Stochastic Linearization implies:

$$f(X_t) = f(X_{t-1}) + f'(x_{t-1})dt$$

and define the error term as:

$$\bar{e} = \bar{X} - X_{eq}$$

Therefore the problem statement reduces to :

$$\min(E[\int_0^T \bar{e}^T \bar{e} dt])_{A(t), b(t)}$$

Now since

$$\bar{e} = (f(x) - A\bar{X}_{eq} - b) \approx (f(x) - AX_{eq} - b)$$

The cost function is defined as:

$$J = \int_0^T E[(f(x) - AX_{eq} - b)^T (f(x) - AX_{eq} - b)] dt$$

Therefore,

$$\delta J = \int_0^T ([\frac{\partial E(e^T e)}{\partial A}] \delta A + [\frac{\partial E(e^T e)}{\partial b}] \delta b) dt = 0$$

Minimization require:

$$[\frac{\partial E(e^T e)}{\partial A}] = 0$$

$$[\frac{\partial E(e^T e)}{\partial b}] = 0$$

$$\Rightarrow 2E[f(x) - Ax - b] = 0$$

$$\Rightarrow \dot{\bar{X}} = E[f(x)] = A\bar{x} + b$$

Similarly from the first inequality:

$$A = E[f(x)x^T] - \bar{x}E[f^T(x)]P^{-1}$$

Now since,

$$\begin{aligned}\dot{P} &= (AP + PA^T + Q) \\ \Rightarrow \dot{P} &= E[f(x)(x - \bar{x})^T] + E[(x - \bar{x})f^T(x)] + Q(t)\end{aligned}$$

Hence we get the final set of differential equations for the propagation of the mean and variance:

$$\begin{aligned}\dot{\bar{X}} &= E[f(x)] \\ \dot{P} &= E[f(x)(x - \bar{x})^T] + E[(x - \bar{x})f^T(x)] + Q(t)\end{aligned}$$

The Fokker-Plank equation gives the time evolution of the probability density function and is commonly used for computing the probability densities of stochastic differential equations. This is also commonly known as Kolmogorov forward equation. The Fokker-Plank equation was first used to give the statistical description of Brownian motion of a particle in a fluid.

In one spatial direction  $x$ , the Fokker-Plank equation for a process with drift  $D_1(x, t)$  and diffusion  $D_2(x, t)$  is :

$$\frac{\partial}{\partial t} f(x, t) = -\frac{\partial}{\partial x} [D_1(x, t)f(x, t)] + \frac{\partial^2}{\partial x^2} [D_2(x, t)f(x, t)]$$

More generally, the time dependent probability distribution function may depend on a set of  $N$  variables  $x_i$ . The general form of the Fokker-Plank equation can then be written as:

$$\frac{\partial}{\partial t} f(x, t) = -\sum_{i=1}^N \frac{\partial}{\partial x_i} [D_i^1(x_1, x_2, \dots, x_N, t)f] + \sum_{i=1}^N \sum_{j=1}^N \frac{\partial^2}{\partial x_i \partial x_j} [D_{ij}^2(x_1, x_2, \dots, x_N, t)f(x, t)]$$

Here  $D^1$  and  $D^2$  are drift and the diffusion tensors respectively. The diffusion term results from the presence of the stochastic forces. Probability density of stochastic differential equations are computed using Fokker-Plank equations. We take the Ito

stochastic differential equation:

$$d\mathbf{X}_t = \mu(\mathbf{X}_t, t)dt + \sigma(\mathbf{X}_t, t)d\mathbf{W}_t$$

This can be understood as the stock price model used by Black and Scholes where  $\mu(\mathbf{X}_t, t)$  represents the instantaneous rate of return on a riskless asset,  $\sigma(\mathbf{X}_t, t)$  is the volatility of the stock, and  $d\mathbf{W}_t$  represents the infinitesimal change in a Brownian motion over the next instant of time. Where  $\mathbf{X}_t \in R^N$  is the state and  $W_t \in R^M$  is a standard M-dimensional Wiener process. If we assume the initial distribution to be  $\mathbf{X}_0 \sim f(\mathbf{x}, 0)$  then the probability density  $f(\mathbf{x}, t)$  of the state  $\mathbf{X}_t$  is given by the Fokker-Plank equation with drift and diffusion terms as :

$$D_i^1(\mathbf{x}, t) = \mu_i(\mathbf{x}, t)$$

$$D_{ij}^2(\mathbf{x}, t) = \frac{1}{2} \sum_k \sigma_{ik}(\mathbf{x}, t)\sigma_{kj}^T(\mathbf{x}, t)$$

Being a partial differential equation(PDE), the Fokker-Plank equation(FPK) can be solved analytically only in special cases. Different numerical techniques are used for computing the PDE's generated by the FPK. This however is computationally faster than the monte carlo technique where the simulation is run for greater number of sample points.

Let us consider the scalar differential equation excited by white noise(W) of unit intensity. We can write the differential equation as :

$$\dot{x} = -x + \epsilon x^3 + W$$

Here W is the white noise of unit intensity and  $\epsilon$  is a parameter. For our computational purposes we are taking the value of epsilon as  $\epsilon = -0.1$ . The value of epsilon is so chosen such that the probability distribution function shows a stable behavior.

We will use the different methods for the propagation of uncertainty and compare the statistics obtained by each of them.

The given differential equation is:

$$\dot{x} = -x + \epsilon x^3 + w$$

Where  $w$  is white noise of unit intensity It is intuitive to write the differential equation as:

$$\Delta x = (-x + \epsilon x^3)\Delta T + \Delta w$$

Now here  $\delta T$  is fixed. We start with a small value of  $\Delta T (= 0.1)$  and run the monte carlo simulation and match the mean and variance with the Gaussian closure method. We are running the simulation for this small period of time though the process can be run for higher time spans by breaking that span into small (smaller!) increments and capturing the statistics accurately and then propagating the states. The end result of the integration for each step would become the initial condition for the next propagation. Matlab goes dismally slow and hence puts the restriction on running these for smaller steps and capturing the accurate dynamics for even higher samples. Though, it is being illustrated here that the dynamics is being captured adequately with even small number of samples. ( $n = 100$  for noise and IC, assumed to be Gaussian).

$$\dot{x} = -x + \epsilon x^3 + W$$

Clearly,

$$f(x) = -x + \epsilon x^3$$

Upon substitution we get the differential equation for the mean and variance:

$$\dot{\bar{X}} = \epsilon(\dot{X})^3 + \bar{X}(3\epsilon P - 1)$$

$$\dot{P} = 2(-P + \epsilon(6\mu^2 P + 3P^2 - 3\mu P)) + Q$$

Here,  $\bar{X} = \mu$  and  $P = \sigma^2$  How does the plot of mean and variance look like??

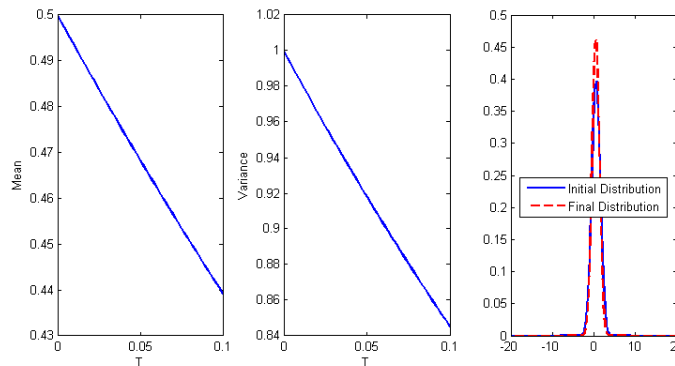


Fig. 21. Evolution of the dynamics using statistical linearization method. The simulation is run with starting statistics of mean 0.5 and variance of 1.

We note here that the simulation is being run for a very small amount of time.  $\delta T = 0.1s$ . Again the value of epsilon is being taken as  $\epsilon = -0.1$ . The plots so obtained is compared with the monte carlo simulations. Figure (21) shows the evolution of mean, variance and distribution on the Initial Condition using the Statistical Linearization Approach. Using the above equation(eqn) we get the partial differential equation of the PDF evolution as:

$$\frac{\partial p(x, t)}{\partial t} = (x - \epsilon x^3) \frac{\partial p(x, t)}{\partial x} + (1 - 3x^2)p(x, t) + \frac{1}{2} \frac{\partial^2 p(x, t)}{\partial x^2}$$

This solution for the PDE satisfies the boundary condition as:

$$p(t, \infty) = p(t, -\infty) = 0$$

We can solve the above equation using Matlab that will give the evolution of the PDF with time and space. The simulation is run for 0.1 secs with  $\epsilon = -0.1$  and with the same initial statistics as in previous cases. This will allow us to compare and contrast the distribution obtained through different methods. The evolution of PDF can now be seen as given in the figure (22).

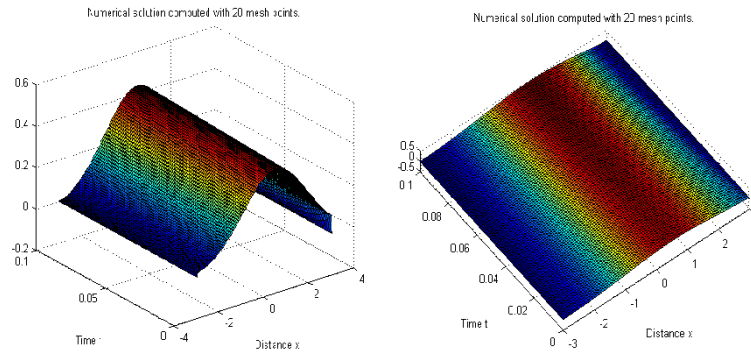


Fig. 22. Evolution of the PDF using the Fokker Plank Equation. The simulation is run with starting statistics of mean 0.5 and standard deviation of 0.01.



## APPENDIX C

## REPRESENTATION OF ARBITRARY RANDOM INPUTS

We know that with appropriately chosen Weiner Askey Polynomial Chaos expansion based on the type of standard arbitrary random inputs, optimal convergence rate of the chaos expansion is realized. However, for most of the cases the distribution of the random input is not of the standard type as given in the table or even if they do belong to certain standard types, the correspondence is not explicitly known. For these cases we need to project the input process onto the weiner askey Polynomial Chaos basis directly in order to solve the differential equation.

For example, let us consider the ordinary differential equation :

$$\frac{dy(t)}{dt} = -ky, y(0) = \hat{y}$$

Now let us assume that the distribution of the decay parameter  $k$  is known in the form of the probability function  $f(k)$ . The representation of  $k$  by the weiner-askey Polynomial Chaos expansion takes the form

$$k = \sum_{i=0}^P k_i \phi_i$$

where,

$$k_i = \frac{\langle k \phi_i \rangle}{\phi_i^2}$$

Where we know from the previous work that the operation  $\langle ., . \rangle$  denotes the inner product in the Hilbert space spanned by the Weiner-Askey chaos basis  $\phi_i$ , ie.,

$$k_i = \frac{1}{\langle k \phi_i^2 \rangle} \int k \phi_i(\xi) g(\xi) d\xi$$

Where  $g(x)$  and  $g(x_i)$  are the probability function of the random variable  $\xi$  in the Weiner-Askey Polynomial Chaos for continuous cases. Here we are taking the assumption that that the random variable  $\xi$  is fully dependent on the target random variable  $k$ . We understand that the support of  $k$  and  $\xi$  are different. This is the other way of saying that  $k$  and  $\xi$  can belong to two different probability spaces  $(\Omega, \Lambda, P)$ , with different event spaces  $\Omega$ ,  $\sigma$  – algebra  $\Lambda$  and probability measure  $P$ .

For us to be able to conduct the above projection we need to transform the fully correlated random variables  $k$  and  $\xi$  to the same probability space. The standard method is to transform them to the uniformly distributed probability space  $u \in U(0, 1)$ . This is the key to random number generation, where the uniformly distributed numbers are generated as the seeds and then the inverse transformation is performed according to the desired distribution function. Let us assume that the random variable  $u$  is uniformly distributed in  $(0, 1)$  and the PDF's for  $k$  and  $\xi$  are  $f(k)$  and  $g(\xi)$  respectively. A transformation of the variable in probability space shows that

$$du = f(k)dk = dF(k), \quad du = g(\xi) = dG(\xi)$$

Where  $F$  and  $G$  are the distribution functions of  $k$  and  $\xi$ , respectively, ie,

$$F(k) = \int_{-\infty}^k f(t)dt, \quad G(\xi) = \int_{-\infty}^{\xi} g(t)dt.$$

If it is desired to convert the random variables to  $k$  and  $\xi$  to be transformed to the same uniformly distributed random variable  $u$ , we obtain

$$u = F(k) = G(\xi)$$

After inverting the above equation we get

$$k = F^{-1}(u) \equiv h(u), \quad \xi = G^{-1}(u) \equiv l(u)$$

By doing so we convert the two random variables  $k$  and  $\xi$  to the same probability space defined by  $u \in$ , the projection (6.2) can be performed as,

$$k_i = \frac{1}{\langle \phi_i^2 \rangle} \int k \phi_i(\xi) g(\xi) d\xi = \frac{1}{\langle \phi_i^2 \rangle} \int_0^1 h(u) \phi_i(l(u)) du$$

It is difficult to evaluate the above integral analytically. However it is possible to evaluate the above integral using the Gauss quadrature in the closed domain  $[0, 1]$  with reasonable accuracy. The analytical form for some of the standard distributions are known. The above process requires that the distribution functions are known and the inverse functions  $F^{-1}$  and  $G^{-1}$  exist and be known as well. In practice this is not always satisfied and we know only the probability function  $f(k)$  for a specific problem. The probability function  $g(\xi)$  is known from the choice of Weiner-Askey Polynomial Chaos but the inversion is not known always. In this case we can perform the projection(6.2) directly by monte carlo integration, where a large ensemble of random numbers  $k$  and  $\xi$  are generated. Further the requirement that  $k$  and  $\xi$  be transformed to same probability space  $U \in (0, 1)$  requires that  $k$  and  $\xi$  has to be generated from the same **seed** of uniformly generated random number  $U \in (0, 1)$ . In this section we present numerical examples of representing an arbitrarily given random distribution. Here, we will try to capture non Gaussian random variables using Hermite Chaos. Although, the solution by Hermite chaos converges but optimal exponential convergence is not realized. It is assumed that the decay parameter  $k$  in the ordinary differential equation is a random variable with exponential distribution with pdf of the form

$$f(k) = e^{-k}, k > 0$$

The inverse of its distribution function is known as

$$h(u) \equiv F^{-1}(u) = -\ln(1 - u), u \in U(0, 1)$$

We now take the Hermite-chaos as the Polynomial Chaos expansion of  $k$  instead of the optimal Laguerre-chaos. The standard random variable  $\xi$  is a standard Gaussian random variable with PDF  $g(\xi) = \frac{1}{\sqrt{2\pi}}e^{-\frac{\xi^2}{2}}$ . The inverse of the Gaussian distribution  $G(\xi)$  is known as

$$l(u) \equiv G^{-1}(u) = -\text{sign}(u - \frac{1}{2})\left(t - \frac{c_0 + c_1t + c_2t^2}{1 + d_1t + d_2t^2 + d_3t^3}\right)$$

Where,

$$t = \sqrt{-\ln[\min(u, 1 - u)]^2}$$

and  $c_0 = 2.515517, c_1 = 0.802853, c_2 = 0.010328, d_0 = 1.432788, d_1 = 0.189269, d_2 = 0.001308$  The above analytical form is taken from Hastings.

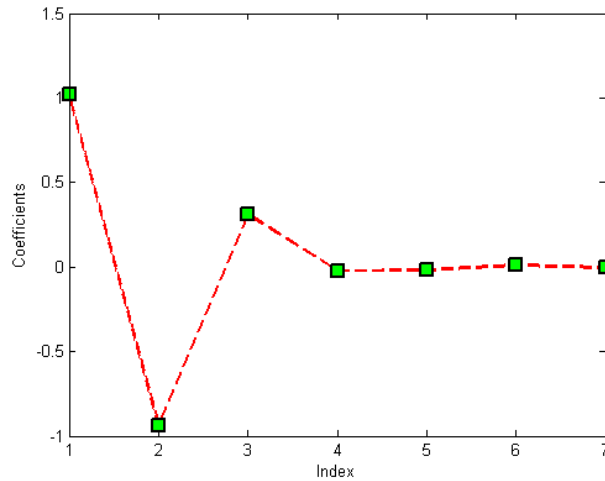


Fig. 23. Numerical values of the coefficients of Hermite Chaos expansion used for capturing exponential distribution.

The figure (23) shows the results when the exponential distribution is captured by the Hermite Chaos. We see that the major contribution of the Hermite chaos expansion is coming from the first three terms.

## APPENDIX D

POLYNOMIAL CHAOS EXPANSION METHOD FOR SOLVING  
UNCERTAINTY IN VAN DER POL EQUATIONS

The Cameron-Martin theorem states that any second-order (i.e, finite variance), one dimensional process  $G$  can be written as the weighted sum of the Hermite polynomials in the Gaussian random variable  $\xi$  (taken to have zero mean and unity variance), and that series converges in the  $L_2$  sense. Using the symbolic notation of Abramowitz and Stegun,

$$G = \sum_{i=0}^{\infty} g_i He_i(\xi)$$

Clearly, the distribution  $G$  is constructed from modes which are Hermite Polynomials:  $He_0 = 1, He_1(\xi) = \xi, He_2(\xi) = \xi^2 - 1, \dots$ . Further, inner product of Hermite polynomials are orthogonal with respect to the Gaussian PDF of the random variable  $\xi$ . i.e.,

$$\int_{-\infty}^{\infty} e^{-\frac{\xi^2}{2}} He_i(\xi) He_j(\xi) d\xi = e_{ij} \delta_{ij}$$

Where  $\delta_{ij}$  are Kronecker delta function. We note that the orthogonality holds when the weight functions are replaced by equivalent PDF of the random variable. Higher tensors can similarly be defined as,

$$\int_{-\infty}^{\infty} e^{-\frac{\xi^2}{2}} He_i(\xi) He_j(\xi) He_k(\xi) d\xi = e_{ijk} \delta_{ijk}$$

We will cite a specific example to illustrate the use of Polynomial Chaos expansion to handle parametric uncertainty. Let us consider the case of van der pol equation,

$$\frac{d^2 y}{dt^2} + \mu(y^2 - 1) \frac{dy}{dt} + y = 0$$

Here  $x$  is the position coordinate which is a function of time  $t$ , and  $\mu$  is a random variable with uniform distribution. The above equation now becomes stochastic in nature. We will illustrate in this example the way Polynomial Chaos method converts the stochastic differential equation into deterministic linear equations in higher dimensions. Let us write the differential equation in the state space form as,

$$\frac{dx}{dt} = y$$

$$\frac{dy}{dt} = \mu(1 - x^2) - x$$

In this problem, the random variable  $\mu$  is expressed as a finite summation of modes, up to the order  $P$ , along with the states. Hence the mathematical form is given as,

$$\mu = \sum_{i=0}^P \mu_i Le_i(\xi)$$

$$y(t) = \sum_{i=0}^P y_i(t) Le_i(\xi)$$

$$x(t) = \sum_{i=0}^P x_i(t) Le_i(\xi)$$

Where  $Le_0 = 1$ ,  $Le_1 = \xi$ ,  $Le_2 = \frac{1}{2}(3\xi^2 - 1)$ ,  $Le_3 = \frac{1}{2}(5\xi^3 - 3\xi)$  are Legendre polynomials and possess the inner product property as Hermite polynomials. Substituting into the dynamic equation we obtain,

$$\sum_{i=0}^P \dot{x}_i(t) Le_i(\xi) = \sum_{i=0}^P y_i(t) Le_i(\xi)$$

$$\sum_{i=0}^P \dot{y}_i(t) Le_i(\xi) = \sum_{i=0}^P \mu_i Le_i(\xi) \left(1 - \sum_{i=0}^P \sum_{j=0}^P x_i(t) x_j(t) Le_i Le_j\right) - \sum_{i=0}^P x_i(t) Le_i$$

Next, using the inner product property of these series of orthogonal polynomials, we multiply by the  $k^{th}$  mode and take the Galerkin projection to obtain a set of deterministic linear equations in higher dimensions:

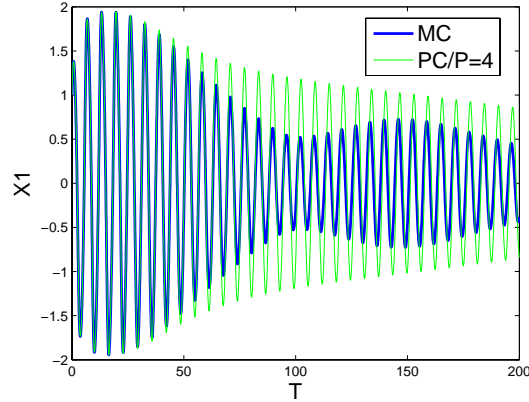


Fig. 24. Evolution of Monte Carlo and Polynomial Chaos trajectory with time. The results match and the divergence over the period of time is due to long term integration issues of Polynomial Chaos method.

$$\begin{aligned}\dot{x}_k(t) &= y_k(t), \\ \dot{y}_k(t) &= \mu_k - \frac{1}{e_{kk}} \sum_{l=0}^P \sum_{j=0}^P \sum_{i=0}^P x_i(t)x_j(t)\mu_l e_{ijkl} - x_k(t)\end{aligned}$$

In the case of no parametric uncertainty ( $\mu_i = 0, i > 0$ ) and without nonlinearity each mode will evolve independent of each other in accordance with the properties of time invariant linear systems.

We observe from figure (24) that the Polynomial Chaos Trajectory matches well with the Monte Carlo Trajectory for initial span of time and diverges after some time because of long term integration issues with Polynomial Chaos Method.



## VITA

Avinash Prabhakar was born in India. He received his baccalaureate degree in aerospace engineering from the Indian Institute of Technology, Roorkee, India in 2002. In August 2002, he joined Tata Steel as a Graduate Engineer Trainee before coming to Texas A&M University on August 2006 for his graduate studies. All graduate level work was performed under the supervision of Dr. Raktim Bhattacharya. His master's thesis focussed on the uncertainty propagation in the hypersonic flight dynamics using Polynomial Chaos Theory.

He can be reached by contacting Dr. Raktim Bhattacharya, Department of Aerospace Engineering, Texas A&M University, College Station, TX 77843-3141.

The typist for this thesis was Avinash Prabhakar.